TECHNICAL MEMORANDUMS

NATIONAL ADVISORY COMMITTEE FOR AERONAUTICS

No. 733

AERODYNAMIC PRINCIPLES OF THE DIRECT LIFTING PROPELLER

By Martin Schrenk

Zeitschrift für Flugtechnik und Motorluftschiffahrt
Vol. 24, Nos. 15, 16, and 17
August 14, August 28, and September 14, 1933
Verlag von R. Oldenbourg, Munchen und Berlin

Washington
January 1934

NATIONAL ADVISORY COMMITTEE FOR AERONAUTICS

TECHNICAL MEMORANDUM NO. 733

AERODYNAMIC PRINCIPLES OF THE DIRECT LIFTING PROPELLER*

By Martin Schrenk

SUMMARY

The purpose of this report is to make the complicated processes on the direct-lift propeller amenable to analysis and observation. This is accomplished by placing the physical phenomena, starting with the most elementary process, in the foreground, while limiting the mathematical treatment to the most essential in view of the fundamental defects of the theorems. Comparison with model experiments supplements and corroborates the theoretical results.

INTRODUCTION

Among the various rotating airfoil systems,** the autogiro, in spite of being the most recent arrival in the series, has been the first to receive general recognition,

---

*"Die aerodynamischen Grundlagen der Tragschraube." Z.F.M., August 14, 1933, pp. 413-419; August 28, 1933, pp. 449-454; and September 14, 1933, pp. 473-481.

**As to the types of rotary airfoil systems, the following definitions are used. Any aircraft with rotating airfoils for producing lift - in contradistinction to aircraft with "fixed" wing systems - falls into this class. At present they may be divided into three different categories:

1) Autogiro: An aircraft having one or more systems of airfoils rotating substantially about a vertical axis; that is, the air flows upward through the propeller disk.

2) Helicopter: An aircraft having one or more sets of airfoils essentially rotating about a vertical axis but driven from the aircraft; that is, the air passes downward through the propeller disk.

3) Cyclogiro (name coined by Dr. Rohrbach): An aircraft having substantially a system of airfoils rotating about a horizontal axis, which can be made to rotate freely in the relative wind or be driven from the aircraft.

thanks to the successful research of Juan de la Cierva. But the development of simple and practical readily applicable scientific principles, has not kept step with it (at least in publicly accessible form).

Admittedly, Glauert (reference 1) and Lock (reference 2) evolved a very detailed mathematical theory in 1926-27; and Lock and Townend (reference 3) published in 1928 the results of elaborate experiments on a model autogiro. But these reports, invaluable as they are, fail to establish a connection between theory and model test. In its particular form, the theory is much too unwieldy for practical application; the meaning of the assumptions and reductions is difficult to survey. The model experiments are limited to one execution and the theory does not permit the application of its data to any other form.

The purpose of the present report is to remove these objectionable features. The road thereto leads through a very much reduced mathematical treatment which reveals the physical aspect much better than attained heretofore. Owing to the complexity of the air flow composed of tip and forward speed, together with the flapping motion of the blades of itself, the processes on the autogiro are such that no clear conception can be obtained unless the most elementary basic notions are put forward first and then the effect of the additional processes is superimposed afterward.

There are two methods of analyzing the autogiro (analogous to driving propellers): one, referring to the processes at the individual blade; the other, comprising the total flow. The latter may be based on the Prandtl airfoil theory and yields the induction losses. But the former gives - after more accurate consideration - aside from the thrust, the flapping motion and its effects and - after suitable simplification - an inferior limit value for the axial flow loss.

Upon comparison with model experiments, it is then found that no rational agreement is possible unless the assumption held heretofore and employed without proof by the British research workers, relative to the form and location of the induced field of flow, is discarded in favor of another admittedly only empirically definable assumption for the present. Then it becomes possible to compute an autogiro from the correct profile drag coefficients of

the blades, in contrast to the conjectured increment employed heretofore, which is diametrically opposed to the mathematical accuracy of the theory.

Lastly, a simple relation is deduced in semi-empirical manner, for the residual loss produced by the unsymmetrical air flow on either side of the principal plane. The representation of these three loss quotas in form of lift/drag ratio proportions, yields a profound insight into the effect of the individual design quantities and gives the designer a yardstick for evaluating the effect of his methods and the attainable limits.

A complemental section briefly discusses divers refinements, strength problems, and the phenomena at high angles of attack.

Notation

Other than the symbols proposed by the subcommittee of the FALU and published in Z.F.M. (Zeitschrift für Flugtechnik und Motorluftschiffahrt), no. 22, 1932, the following are employed.

Dimensions of blades:

F, disk area of autogiro.

R, radius of autogiro,

r, radius of blade element.

t, chord of blade.

m, weight of blade per unit length.

J, inertia moment of blade about hinge.

z, number of blades.

σ, surface density, or solidity ratio $\left(\frac{ztR}{F}\right)$, with t = chord at r = R.

Forces:

L, air force (general).

S, thrust (resultant force) of autogiro.

T, tangential force (in plane of propeller).

M, moment of T.

M_s, moment of S.

k_s, thrust coefficient $\left(\frac{S}{\frac{\rho}{2} u^2 F}\right)$

c_s, resultant force coefficient,* $\left(\frac{S}{\frac{\rho}{2} v^2 F}\right)$ (identical to c_r on airplane wing).

Motion:

u, tip speed (at $r = R$).

v_d, axial velocity (due to permeability of autogiro).

w, induced deflection velocity at the locus of the propeller.

c, resultant air-flow velocity at blade element (c_x and c_y components).

ω, rotational speed.

λ, tip-speed ratio $\left(\frac{v \cos \alpha}{u}\right)$

λ_d, coefficient of axial flow $\left(\frac{v_d}{u}\right)$.

Angles:

α, angle of attack of normal plane.

---

*In propeller theory c_s is the load factor, but since it assumes here the role of the resultant force coefficient at the airfoil, it is called such, to differentiate it from the thrust coefficient k_s.

Angles (contd.):

ϑ, blade angle (incidence of blade element to normal plane).

φ, angle of flow at blade relative to normal plane.

ψ, turning angle of blade (zero position aft).

β, flapping angle (relative to normal plane).

Constant values:

ζ, coefficient of flow.

κ, coefficient of nonuniformity loss.

γ, comparative factor for dynamic similitude $\left(\frac{\frac{\rho}{2} c_{ap} t R^4}{J}\right)$

$\left.\begin{matrix} m \\ p \end{matrix}\right\}$, geometrical constants.

Subscripts:

p, blade profile (c_{ap}, α_p, ϵ_p).

d, axial flow (v_d, λ_d, α_d, ϵ_d).

i, induced (α_i, ϵ_i).

u, nonuniformity (ϵ_u).

THE AUTOROTATING WINDMILL

Everybody remembers the toy windmill of his childhood, the original autorotating windmill. It is well to consider for a moment the process involved. Figure 1 illustrates a blade element $t\,dr$ of an autogiro, which is only to revolve at distance r about the axis of rotation. There being no input nor output in this elementary windmill, the resultant force $d\,S$ as well as the velocity of axial flow v_d through the normal plane is at right angles to it. The

manner in which v_d depends on external circumstances is for the time being, disregarded.

Then, figure 1 reveals

$$\tan \varphi = \frac{v_d}{r\omega} = \lambda_d = \frac{d\ W_p}{d\ A}$$

or

$$\lambda_d = \epsilon_p \qquad (II,1)$$

The axial flow coefficient $\lambda_d = \frac{v_d}{u}$ is by nature identical with tip speed ratio $\lambda = \frac{v}{u}$ and becomes so much smaller as the lift/drag ratio of the profile is better.

Now, how must the blade be set to insure the highest possible thrust under any given axial velocity v_d?

It is

$$d\ S = \frac{\rho}{2}\, c_{ap}{}^2\ u\ t\ dr = \frac{\rho}{2}\, c_{ap}\, \frac{v_d{}^2}{\lambda_d{}^2}\ t\ dr$$

or

$$\frac{d\ S}{\frac{\rho}{2}\, v_d{}^2\ t\ dr} = \frac{c_{ap}}{\lambda_d{}^2} = \frac{c_{ap}}{\epsilon_p{}^2} = \frac{c_{ap}{}^3}{c_{wp}{}^2} \qquad (II,2)$$

In other words, with constant v_d the thrust depends on the well-known profile characteristic (criterion of climb) $c_a{}^3/c_w{}^2$.

The angle of attack of the profile α_p (which defines the lift of the profile) is composed, according to figure 1, of the angle of flow $\varphi (= \lambda_d)$ and the fixed blade incidence ϑ. Thus (II,1) gives

$$\epsilon_p = \alpha_p - \vartheta \qquad (II,3)$$

with normal blade incidence, angle α_p is solely dependent upon ϵ_p. This means that the choice of blade angle ϑ with given profile at the same time establishes the lift coefficient c_{ap}, which the rotating blade maintains during steady attitude independent of the loading.

Equation (II,3) lends itself very readily to graphic

representation (fig. 2). By plotting ϵ_p in degrees of angle against α_p and ϑ on the α_p-axis, the straight line drawn from the end of ϑ with 45-degree slope gives all steady and accelerated attitudes possible with this blade angle. The elementary windmill is accelerated at all angles between points 1 and 2; at point 1 it has its steady, stable turning attitude, beyond point 2 it is quickly decelerated.

This decrease of revolution upon exceeding a stated operating angle of the blade is typical of the autorotation. The process is analogous to the concept of spinning insofar as the rotation in both cases must be initiated by an outside impulse; but for the rest, it is unlike the other, since there is no angle of attack beyond the maximum lift on the autorotating elementary windmill.

The autogiro of constant axial velocity.- In passing from the element to the whole propeller, we must first determine the form and thereby the flow conditions. But instead of choosing the habitual rectangular blade form and coordinating arbitrarily a certain distribution of the axial velocity, we attempt to find a form with possibly simple distribution of lift coefficient and axial velocity. Since, according to the foregoing, the quality of the resultant thrust is contingent upon the expression $\frac{c_{ap}^3}{c_{wp}^2}$, that is, on c_{ap}, it is advisable to choose c_{ap} = constant, attainable when v_d is known by twisting the individual blade elements with respect to each other. It is also desirable to have v_d = constant for reasons of mathematical simplicity. This grading with given total quantity of axial flow per second corresponds, moreover, to a minimum of kinetic power loss.

Disregarding the boundary effects, the autorotating propeller may then be considered as a stream section through which the air passes with the positive pressure S/F. Obviously the flow resistance in this section resolves itself according to the proportion of the thrust produced at the pertinent point; the resistance and through it, the speed are constant across the whole section, even with uniform thrust grading. The result is therefore the same simple thrust grading as with the axial theory of the propeller.

Outwardly, however, a uniform thrust grading across the section means a linearly increasing thrust loading of the individual blade:

$$\frac{d\,S}{d\,r} \sim r.$$

This grading is obtained with c_a = constant, when choosing chord t conformably to

$$t \sim \frac{1}{r}.$$

Then

$$\frac{d\,S}{d\,r} \sim r^2\,t \sim r.$$

Admittedly, this equation leads to forms for which the blade chord increases to ∞ on the axis; besides, the blade angles deviate so much from the propeller plane in the vicinity of the axis, that c_a is no longer decisive for the locally produced thrust ($\cos\varphi$ is no longer ≈ 1). On the other hand, the proportion of the blade near the hub to the thrust produced is so small (not exceeding 2 to 3 percent for a propeller of figure 3), as to be safely neglected, especially as the axial flow in the propeller center is, apart from that, disturbed by the more or less large hub.

The decrement of the thrust at the boundary can also be summarily disregarded for, as seen directly, the flow coefficient of the air passing through is unusually low; the individual propeller surfaces thus follow each other very closely.

Thrust and axial flow coefficient.- In contrast to the elementary autogiro, the resultant air force L (fig. 4) on the different parts of the blade of the steadily autorotating propeller is now no longer perpendicular to the plane of rotation, but slopes forward in the direction of rotation at the inside elements and backward at the outside elements. Thus, those on the inside act in a propellent manner, those on the outside, are propelled; somewhere between lies a blade portion which still corresponds to the simple elementary conception.

In the most important part of the blade the angle $(\varphi - \epsilon_p)$ (fig. 4) is apparently of the order of ϵ_p.

that is, very small, so that φ remains small also. In consequence, the small thrust component of the profile drag ($d W_p \sin \varphi$) can be disregarded and the thrust element be expressed with

$$d S = d A \cos \varphi = \frac{\rho}{2} c_{ap} v_{res}^2 t \, d r \cos \varphi$$

$$= \frac{\rho}{2} c_{ap} r^2 \omega^2 t \, dr \frac{1}{\cos \varphi}$$

With $\cos \varphi = 1$, we then have

$$d S = \frac{\rho}{2} c_{ap} r^2 \omega^2 t \, dr$$

According to the preceding chapter, the wing chord at point r is

$$t = t_R \frac{R}{r} \qquad (II,4)$$

and the thrust of z blades

$$S = z \int_0^R d S = z \frac{\rho}{4} c_{ap} \omega^2 R^3 t_R .$$

Lastly we put

$$z R t_R = \sigma F \qquad (II,5)$$

wherein σ = solidity, that is, the ratio of the z rectangles of minimum chord times radius to propeller disk area F. Then the thrust is

$$S = \frac{\rho}{4} \sigma c_{ap} u^2 F = \frac{\rho}{2} k_s u^2 F \qquad (II,6)$$

where the thrust coefficient referred to tip speed is

$$k_s = \frac{\sigma c_{ap}}{2} \qquad (II,7)$$

Since, according to (II,3), c_{ap} (α_p) with given blade form is a constant value independent of the load, k_s is also simply a function of the blade form.

The axial flow coefficient λ_d follows from the con-

dition that no free moment occurs with the autorotating propeller. With the notations of figure 4, the component of the tangential force is

$$d\,T = A \sin\varphi - d\,W_p \cos\varphi$$

$$= \frac{\rho}{2} \frac{r^2\,\omega^2\,t\,dr}{\cos^2\varphi} (c_a \sin\varphi - c_{wp} \cos\varphi).$$

The division of the brackets by $\cos^2\varphi$ and by $\cos\varphi = 1$ together with equation (II,4), yields

$$d\,T = \frac{\rho}{2}\, r\,\omega^2\, R\, t_R\, dr \left(\frac{v_d}{r\omega} c_a - c_{wp}\right) \qquad (II,8)$$

while (II,5) gives the moment at

$$M = z \int_0^R r\,d\,T = \frac{\rho}{2}\,\sigma\, c_{ap}\, R\, u^2\, F \left(\frac{\lambda_d}{2} - \frac{\epsilon_p}{3}\right) \qquad (II,9)$$

and by putting $\lambda_d = 0$,

$$\underline{\lambda_d = \frac{2}{3}\,\epsilon_p.} \qquad (II,10)$$

This formula states that the outside 1/3 of the propeller is driven by the inside 2/3. When plotting this formula (10) conformably to figure 2, the angle of attack α referred to a stated incidence ϑ can be obtained for the selected profile. But the values do not apply to extreme radius R, but to point $r = \frac{2}{3}R$. Figure 5 shows the values for the Göttingen airfoil 429.

Axial velocity v_d.- Now, formulas (II,6) and (II,10) would yield the axial velocity v_d as function of surface loading S/F, the surface density α and the aerodynamic characteristic. But we prefer to follow a different route which brings the physical aspect of the axial velocity into better relief.

From a glance at figure 4, it becomes apparent that the components of the lifting forces against the profile drag maintain the autorotation. Without this drag the rotation would increase arbitrarily. Now the power necessary to overcome the profile drag must be produced somehow; it is supplied by the quantity of air $v_d\,F$ passing through the section per second at positive pressure S/F.

Formula (II,9) gives the moment of the profile drag at

$$M_p = \frac{\rho}{6} \sigma c_{wp} R u^2 F$$

and the power of the profile drag at

$$N_p = M_p \omega = \frac{M_p u}{R} = \frac{\rho}{6} \sigma c_{wp} u^3 F.$$

Inserting v_d from (II,10) and equating the whole to the power $S v_d$ of the passing air, gives:

$$N_p = \frac{9}{16} \rho \sigma \frac{c_{ap}^3}{c_{wp}^2} F v_d^3 = S v_d.$$

Whence the axial velocity:

$$v_d = \frac{4}{3} \sqrt{\frac{S/F}{\rho \sigma \frac{c_{ap}^3}{c_{wp}^2}}} \qquad (II,11)$$

But this is simply a kind of axial flow formula:

$$v_d = \zeta \sqrt{\frac{S/F}{\rho/2}} \qquad (II,12)$$

with axial-flow coefficient:

$$\zeta = \frac{4/3}{\sqrt{2 \sigma \frac{c_{ap}^3}{c_{wp}^2}}} \qquad (II,12)$$

The autorotating propeller can be considered as a circular stream section, a kind of diaphragm, through which the air passes at pressure S/F. But owing to the resistance existing in the section only the ζ-fold* mass passes through rather than the mass $\rho v_d F$ per second, corre-

*In practice, the order of magnitude of ζ ranges between $\zeta = 0.12$ and 0.25.

sponding to S/F. The smaller the absorption of profile power by the propeller while revolving, the smaller ζ is, and the more "dense" the propeller. Formula (II,12) shows that the profile characteristic sets up limits for c_{ap}^3/c_{wp}^2; practical reasons prevent arbitrary enlargement of σ.

Lastly, the tip speed is obtained from (II,11) and (II,10) at

$$\frac{v_d}{\lambda_d} = u = 2\sqrt{\frac{S/F}{\rho\ \sigma\ c_{ap}}} \qquad (II,13)$$

The greater $\sigma\ c_{ap}$ is, the smaller ζ (II,12) is, the more "dense" the propeller, but so much lower the tip speed.

AUTOGIRO OF LOW TIP-SPEED RATIO

Now we shall see to what extent the just evolved formulas for the autorotating propeller may be utilized on the autogiro in level flight.

Mechanism of lift.- Lift, that is, a force transverse to the air flow, is always the result of stream deflection. At the locus of the lift generatrix in the usual cases wherein it can be represented by one single lifting vortex, this deflection has precisely reached one half of its final amount. The latter is readily computed for uniform distribution from the lift, or, more rigorously, from the resultant air load L. Prandtl's airfoil theory gives the angle of deflection α_i of the flow at the locus of the wing at

$$\sin \alpha_i\ (\approx \alpha_i) = \frac{w}{v} = \frac{L}{\pi \frac{\rho}{2} v^2 b^2} = \frac{c_L}{\pi} \frac{F}{b^2} \qquad (III,1)$$

wherein w is the deflection component of the flow at the locus of the lift generatrix lying in the direction of L, and c_L the coefficient of L.

Thus far the analysis has been equally applicable to a fixed-wing system, a direct lifting propeller as well as to any other lift-producing mechanism. But the setting

with angle α_i does not generally suffice to produce air load L.

On the fixed wing, for instance, the profile must further be rotated through the profile setting angle α_p, to insure the necessary circulation for L. Its amount is computed from the lift curve with slope $dc_a/d\alpha_p$, whose theoretical value is 2π; owing to boundary layer losses $dc_{ap}/d\alpha_p$ drops to from 5.5 to 5.9, according to the Reynolds Number.

These facts are of themselves well known. They are merely repeated here as a reminder incidental to the transition to the lifting propeller.

One can no longer speak of a profile setting angle for the lifting propeller as a whole as with the fixed-wing system, because the process of lift production occurs at the individual blade elements. But its place is taken by another additional angle, the angle of flow α_d (fig. 6).

Autogiro tip-speed ratio approaching zero.- When on the autogiro exposed at small angle to the air stream (fig. 6), the air forces are applied at the individual blade, the asymmetry in magnitude and direction of the resultant flow at the advancing and retreating blade leads to quite complicated formulas so long as the air-stream velocity is of the same order of magnitude as the tangential velocity. One is then tempted to strike out inconvenient terms during the calculation, without fully realizing the effect of such procedure - a danger which Glauert (reference 1) likewise did not avoid.

On the other hand, the matter becomes immediately more simplified and amenable to survey when limited to the attitude of very low tip-speed ratio:

$$\lambda = \frac{v \cos \alpha}{u} \qquad \text{(III,2)}$$

or, in other words, by assuming the forward speed $v \cos \alpha$ as very small compared to tip speed u. Then the effect of $v \cos \alpha$ on the blade forces is mitigated and the tangential velocity $r\omega$ is the sole criterion in first approximation.* In this manner the symmetry of the flow on

*Mathematically this is equivalent in broad outlines to an omission of $(v \cos \alpha)^2$ in the squared sum $(r\omega \pm v \cos \alpha)^2$, which then becomes $r^2 \omega^2$.

the lifting propeller is reestablished and the approximation then yields the same formula as for the autorotating propeller in axial flow (see section "The Autorotating Windmill," page 5), which can be employed forthwith.

We thus apply the picture of the slightly permeable circular disk, on which the air, because of the S/F pressure flows at v_d through the propeller disk in order to maintain autorotation, to the case of oblique air stream also. The aforementioned flow angle α_d is then found, according to figure 6, from the forward velocity $v \cos \alpha$ and the axial velocity v_d as temporarily assumed constant figure for the whole circular surface precisely as the angle of deflection α_i.

Theory of thrust of the "ideal" autogiro.- In connection with the foregoing, an "ideal" lifting propeller is a propeller with its tip-speed ratio approaching zero; that is, of high rotative speed which, in addition, as the result of suitable design shape manifests constant axial velocity across the entire section (lancet shape). This can be readily expressed by a simple theory of the resultant force coefficient

$$c_s = \frac{S}{\frac{\rho}{2} v^2 F} \qquad \text{(III,3)}$$

in terms of angle of attack, with the simple assumption that the total force S is to lie at right angle to the plane of rotation, i.e., in direction of the axis of rotation.

According to figure 6,

$$\sin \alpha = \frac{w + v_d}{v} = \frac{w}{v} + \frac{v_d}{v} \qquad \text{(III,4)}$$

Under the temporarily accepted assumption (as made by Glauert (reference 1) and Lock (reference 2)), that the induced flow at the locus of the wing is plane and has the inclination α_i (III,1) known from Prandtl's theory of the lifting vortex, equation (III,3) yields:

$$\frac{w}{v} = \frac{c_s}{4} \qquad \text{(III,5)}$$

with (II,12), we have further,

$$\frac{v_d}{v} = \zeta \sqrt{c_s} \qquad \text{(III,6)}$$

and finally, with (III,4),

$$\sin \alpha = \frac{c_s}{4} + \zeta \sqrt{c_s} \qquad \text{(III,7)}$$

This is the desired connection. For the range within which one may put $\cos \varphi = 1$, we find:

$$\alpha_i = \frac{c_s}{4} \quad \text{and} \quad \alpha_d = \zeta \sqrt{c_s} \qquad \text{(III,8)}$$

According to this the induction losses increase with c_s, the axial flow losses with $\sqrt{c_s}$. We shall come back to this later.

Lastly, formula (III,7) gives, after resolving the squared equation in $\sqrt{c_s}$, the resultant force coefficient

$$c_s = 4 \left(\sqrt{\zeta^2 + \sin \alpha} - \zeta\right)^2 \qquad \text{(III,9)}$$

After the remark made incidental to (II,8), $k_s = \frac{S}{\frac{\rho}{2} u^2 F_s}$ here also because of the symmetry of the flow. In practice, this means that, with given form of rotating blade, the tip speed is only dependent on surface loading and air density (as is the case in close approximation on actually built autogiros).

Comparison with model experiments.- The only model experiments which by nature and scope are acceptable for comparison with the theory, are those of Lock and Townend (reference 3). The part of the tests referred to here pertains to model blades of 1.80 m (6 ft.) diameter, of wood, constant chord of 136 mm (5.36 in.), without twist, equivalent to a surface density of $\sigma = 0.19$.* The model was tested up to approximately 20° angle of attack; no higher angles were possible in the Duplex wind tunnel of 2.1 by

*The geometrical aspect of σ is not the same for the lancet as for the rectangular blade. Only the relation with the blade chord at the tip is the same in both cases.

4.2 m (7 by 14 ft.) section without introducing serious errors. At a tip speed of around 65 m/s (145 mi./hr.), the profile characteristic on the particular radius 2/3 R" is in fair accord with the normal characteristic of the Göttingen profile measurements. The shape was the symmetrical Göttingen section 429 of 0.10 thickness ratio, modified to give a thicker trailing edge, so that the drag figures are perhaps a little higher than in the Göttingen measurements. But in spite of these minor limitations, the measurements are well suited for comparison with the theory.

Of course, it is not summarily possible to effect such comparison with the lancet-shaped plan form used heretofore in the analysis. At what value shall we put ζ?

So we first assume the formula expressed in (III,7) and (III,9) to be true, i.e., that this equation interprets the form of the $c_s(\alpha)$ curve correctly. This assumption is legitimate because the nonuniformity of the air flow disregarded in the derivation, while being able to affect the direction, cannot, however, influence the amount of the resultant thrust S very substantially.

Therefore we determine by trial or insertion of an experimental value, the coefficient of axial air flow ζ at which the theoretical curve is in closest agreement with the test points. Figure 7 shows the result for blade angle $\vartheta = 1.8^{\circ}$.* The model was measured at this angle for the 4-blader ($\sigma = 0.19$) and the 2-blader ($\sigma = 0.095$) autogiro. The graph shows that the trend of the curve as well as the theoretically stipulated relation $1:\sqrt{2}$ is fulfilled for ζ(II,12). Moreover, this accord holds not only for low tip-speed ratio (great c_s) but also for the highest λ recorded ($\lambda = 0.5$ to 0.6).

From this one is led to infer that certain premises set up in the preceding section have been confirmed. In fact, Lock and Townend (reference 3) conclude from the exact extrapolation for varying blade numbers that the assumption relative to the inclination and the smoothness of the induced field of flow is correct. We shall see hereinafter, to what extent this actually holds true.

But first we examine the conditions of flow and forces of the rectangular blade.

---

*The British text gives hereto, $c_s = 2 L_v \sqrt{1 + \epsilon^2}$.

Thrust and coefficient of flow of autogiro with rectangular blade.- The characteristics of the propeller with rectangular blade are:

$$t = \text{constant} \quad \text{and} \quad \vartheta = \text{constant}$$

But owing to the changeability of tip speed and axial velocity along the radius, the angle of the air stream φ (fig. 1), and through it α_p and c_{ap} are no longer constant.

As concerns the axial velocity v_d, it may be said as before, that it will be constant when the thrust is evenly graded. In reality, however, this occurs only when $\vartheta = 0$, because then

$$\alpha_p = \varphi - \text{constant } \frac{1}{r},$$

that is, the lift increases as a result in inverse ratio to the radius. As ϑ increases, the outside thrust rises faster than on the inside; that is, the flow at the profile is more strongly deflected on the outside and the axial velocity is thereby reduced against that on the inside. No prediction can be made about the actual trend of $v_d = f(r)$ without including the mutual interference, and such calculations would exceed the bounds of this report; although this abstract uncertainty was one of the very reasons which led to the propeller of constant axial velocity used at the beignning of the report.

On the other hand, in order to be able to make any prediction whatsoever, about the rectangular blade, some plausible assumption is necessary, and so we assume with Glauert (reference 1) that v_d is a constant value.

Then the thrust equation is as before

$$d S = \frac{\rho}{2} c_{ap} r^2 \omega^2 t \, dr.$$

Herein

$$c_{ap} = c'_{ap} \alpha_p$$

$$\alpha_p = \vartheta + \varphi = \vartheta + \frac{v_d}{r\omega},$$

consequently,

$$c_{ap} = c'_{ap}\left(\vartheta + \frac{v_d}{r\omega}\right) \qquad \text{(III,10)}$$

which, with (II,5) gives the thrust of z blades at

$$S = z \int_0^R d\,S = \frac{\rho}{2} c'_{ap}\,\sigma\,u^2\,F\left(\frac{\vartheta}{3} + \frac{\lambda_d}{2}\right) \qquad \text{(III,11)}$$

The coefficient of flow is again computed from the condition that $M = 0$. It is

$$d\,T = \frac{\rho}{2} r^2\,\omega^2\,t\,dr\left[\frac{v_d}{r\omega} c'_{ap}\left(\vartheta + \frac{v_d}{r\omega}\right) - c_{wp}\right] \qquad \text{(III,12)}$$

and

$$M = z \int_0^R r\,d\,T = \frac{\rho}{2}\,\sigma\,R\,u^2\,F$$

$$\left[\frac{1}{3}\lambda_d\,c'_{ap}\,\vartheta + \frac{1}{2}\lambda_d^2\,c'_{ap} - \frac{1}{4}c_{wp}\right] \qquad \text{(III,13)}$$

With $M = 0$, one obtains the equation of definition for the coefficient of axial flow

$$\lambda_d^2 + \frac{2}{3}\lambda_d\,\vartheta - \frac{1}{2}\frac{c_{wp}}{c'_{ap}} = 0 \qquad \text{(III,14)}$$

Glauert (reference 1) obtains the same formula by reducing the general equations (λ great) from mathematical reasons, but wherein the physical meaning of this reduction is not forthwith recognizable. Then he puts $c'_{ap} = 6$, although it should be $c'_{ap} = 5.6$ for the ambit of the model experiments. Then

$$\lambda_d = \frac{1}{3}\left(\sqrt{\vartheta^2 + 0.8\,c_{wp}} - \vartheta\right) \qquad \text{(III,15)}$$

Now c_{wp} should not be summarily assumed to have a constant value, because c_{ap} ranges through all possible values across the radius, and c_{wp} is definitely not independent of c_a, especially on symmetrical profiles. Even though the outer half of the blade defines thrust and torque preponderately, and c_{wp} still remains sensibly constant, we nevertheless, introduce, for purposes of more exact investigation, a parabolic relationship $c_{wp} = f(c_{ap})$, of the form

$$c_{wp} = c_{wp_o} + m\, c_{ap}^2$$

and write it in (III,12) for the tangential force. The elementary, albeit somewhat tedious, calculation leads, after inconsequential omissions, to the equation of definition

$$\lambda \frac{2}{d} + \frac{2}{3} \lambda_d \vartheta (1 - m\, c'_{ap}) - \frac{c_{wp_o} + m\, c'^2_{ap}\, \vartheta^2}{2\, c'_{ap} (1 - m\, c'_{ap})} = 0$$

or, with $c'_{ap} = 5.6$, to

$$\lambda_d = \frac{1}{3} (1 - 5.6\, m) \left(\sqrt{\vartheta^2 + 0.8 \frac{c_{wp_o} + 31.4\, m\, \vartheta^2}{(1 - 5.6\, m)^3}} - \vartheta \right) \quad \text{(III,16)}$$

Comparison of rectangular-blade propeller with the model experiments.- From these deduced relations for S and λ_p the connection between c_s and α could be established in the same way as previously for the "ideal" propeller, but the ensuing formula would be rather complicated for a theory of the first order. For this reason we shall proceed in a different direction which, at the same time brings out the connection between the two blade forms.

The purpose of the investigation is to ascertain the profile drag coefficient for the rectangular blade propeller of stated dimensions, which corresponds to a definite figure of merit, according to figure 7. The conception of "equivalent lifting propeller" yields the desired connection. "Equivalent" obviously means: equal axial velocity at equal positive pressure, that is, v_d and S/F are equal. But it does not signify the same λ_d, because the rotative speed may be altogether different by equal permeability, according to the blade form.

With (II,6) and (III,11), in conjunction with $u = \frac{v_d}{\lambda_d}$, we write:

$$S = \frac{\rho}{4} c_{ap}\, \sigma\, F \frac{v_d^2}{\lambda_d^2} = \frac{\rho}{2} c'_{ap}\, \sigma\, F \frac{v_d^2}{\lambda_d^2} \left(\frac{\vartheta}{3} + \frac{\lambda_d}{2} \right)$$

The left-hand side is for the lancet blade, the right-hand side for the rectangular blade. In accord with the assumption, S, F, and v_d are equal and cancel out, but σ and λ_d are not equal. λ_d and ϵ_v must be substituted on the left-hand side, according to (II,10). Then

$$\sigma \frac{c_{ap}^3}{c_{wp}^2} = \frac{8}{9} \zeta^2 = \frac{8}{9} \frac{\sigma c'_{ap} \left(\frac{\vartheta}{3} + \frac{\lambda_d}{2} \right)}{\lambda_d}$$

or

$$\zeta = \frac{\lambda_d}{\sqrt{\sigma c'_{ap} \left(\frac{\vartheta}{3} + \frac{\lambda_d}{2} \right)}} \qquad \text{(III,17)}$$

This equation gives ζ as function of σ, c_{ap}, ϑ and λ_d for the rectangular-blade propeller (λ_d from equation (III,15) or else $\gamma_d = f(\zeta)$.

The evaluation of parabolic profile drag polars is best effected by defining λ_d with assumed values of c_{wp_o} and m from (III,16), followed by insertion in (III,17).

The numerical interpretation is based on the 4-blade model with $\vartheta = 1.8^o$, which gave $\zeta = 0.178$ (fig. 7). With this figure, equation (III,17 and 14) gives the constant profile drag coefficient

$$100\ c_{wp} = 1.65.$$

But the anticipated figure lies at 1.0, according to the polar of the profile Göttingen 429 (fig. 8), having regard to the thickened trailing edge. The models with smaller ϑ manifest a still higher c_{wp}.

Now, one could assume that the increment of profile drag with reduced radius be responsible for this discrepancy. Whether this view is correct, can be seen when combining (III,16) and (III,17). By suitable choice of m we obtain for $\zeta = 0.178$, for instance, the profile polars $100\ c_{wp} = 1.3 + 2.4\ c_a$, shown in figure 8. So the discrepancy of c_{wp} cannot be explained in this manner, at least.*

*To enlarge Glauert's rule of thumb formula c_{wp}, (reference 1) by 50 percent, can hardly be considered an expedient.

The situation is therefore, as follows: The visualization of the autogiro of small tip-speed ratio portrays the type of lift curve $c_s(\alpha)$ in a very elementary formula. But the profile drag figures computed therefrom are considerably higher than anticipated.

So for the present, we analyze the lifting propeller of large tip-speed ratio and the phenomena of "flapping motion."

THE AUTOGIRO OF LARGE TIP-SPEED RATIO - FLAPPING MOTION

As soon as the forward speed $v \cos \alpha$ ceases to be small against the speed $r\omega$ of the outer blade elements within the circle of rotation, the blade thrust on either side of the median plane of the autogiro differs considerably and induces a rolling moment which increases as the tip-speed ratio. The incipient rotation about this axis further causes, so long as the blades are fixed at the hub, a pitching moment as a result of gyroscopic coupling.

La Cierva had some experience with these disagreeable and dangerous moments in his first flight tests in 1922 (reference 4), and that gave him the idea of hinging the blades.* This has proved so satisfactory that almost all autogiros built since have hinged blades. For this reason, we shall limit the investigation to this design, especially since it can be proved that the case of a variable blade angle is identical with it as soon as the axes are correctly chosen.

The hinged autogiro obtains its rigidity simply through the centrifugal forces of the blades. Because of the equilibrium of thrust and centrifugal force, the blades form when revolving a flat coning envelope. The unsymmetry of the air forces affects the shape and position of this cone, and this in turn modifies the spatial angle of air stream of the blades.

---

*But there are other methods of equalizing the effects of unequal lift between the advancing and the receding blade as, for instance, shown in the Wilford gyroplane (reference 5), built according to the patents of W. Rieseler. The opposite blades on either side are rigidly connected together, but free to feather about an axis substantially coincident with the longitudinal axis of the blades themselves.

In view of this complicated condition, it is impossible to reach our aim without effecting certain simplifications in the mathematical analysis.

Autogiro with very heavy blades.- In the processes just indicated the motion of the blades about their root hinge in the plane through the axis of rotation is, of course, of primary importance because of the unequal air flow. This is the so-called "flapping motion." It is not appreciably affected by the "coning motion" so long as the generating coning angle does not differ appreciably from 90°. In actual practice the difference is from 8 to 10°. It is obvious that at first its effect on the calculation should be neglected.

This can be achieved by visualizing (reference 2) the blades as being encumbered with very much weight, so that the centrifugal force becomes great compared to the aerodynamic force. These heavy blades are not to be subject to gravity.* Under the effect of an axially symmetrical air stream such a blade will move in the plane perpendicular to the axis of rotation; its coning angle will be negligibly small.

As soon as periodically changing forces begin to act on such a system characterized by weight and directional force, it results in oscillations. Liebers (reference 6), in his investigation on propeller vibrations, proved that the natural frequency of a propeller with hinged blades is exactly equal to the revolution when the hinges lie on the axis of rotation. And since this is so in nearly every case, we shall assume it also in the following.

The blade oscillates at its natural frequency when the exciting force likewise has the frequency of the revolutions as, in fact, is the case with the thrust forces. Judged from their connection with the angle of rotation, they might be of the nature of harmonics.

Then the situation is as follows: The blades lying on the principal plane, i.e., in flight direction, manifest equal mean aerodynamic forces for reasons of symmetry. The advancing blade dodges the increasing thrust up-

*This limitation is necessary because of the changing magnitude and distribution of the aerodynamic forces on the blade.

wardly; this flapping motion is damped by the ensuing angle-of-attack decrease, and becomes thus comparable to the additional force, that is, highest in pitching. The opposite applies to the retreating blade. We therefore may expect the individual blade to move sensibly in a plane inclined relative to the original plane of rotation, and specifically, under the established assumptions about the axis of pitching (fig. 9).

Equation of flapping motion.- The mathematical analysis of this generalized motion is largely based on Glauert (reference 1) and Lock (reference 2), but with the following simplifying assumptions: The blade (bending-resistant and straight) is evenly loaded with mass m per unit length. Then the dynamic equilibrium of the moments about the hinge at each angular blade setting ψ in flapping motion is

$$\int_0^R r \, dS = \int_0^R m \, r \, \omega^2 \, \beta \, r \, dr + \int_0^R m \, r^2 \, \frac{d^2\beta}{dt^2} \, dr \qquad (IV,1)$$

Moment of thrust = moment of centrifugal force + mass moment of inertia.

By integrating the right-hand side, the moment of thrust (J = inertia moment of a blade about the hinge axis) becomes:

$$M_S = J \left(\frac{d^2\beta}{dt^2} + \beta \, \omega^2 \right) \qquad (IV,2)$$

Then the flapping motion of the blade is expanded as a Fourier series in ψ:

$$\beta = \beta_0 - \beta_1 \cos (\psi - \psi_1) - \beta_2 \cos 2 (\psi - \psi_2) - \ldots$$

$$- \gamma_1 \sin (\psi - \varphi_1) - \gamma_2 \sin 2 (\psi - \varphi_2) - \ldots \qquad (IV,3)$$

This general equation of the flapping motion can be materially simplified by applying the previously cited physical approximation. To begin with, we retain only first harmonics and so reduce the spatial flapping motion to a simple plane motion. Since, in addition, the lateral inclination of the plane of rotation is neglected, i.e., ψ is computed from the rear point of the symmetry, the formula reduces to

$$\beta = \beta_0 - \beta_1 \cos \psi \qquad (IV,4)$$

This is written in (IV,2), whereby $\frac{d\psi}{dt} = \omega$. Then

$$M_s = \beta_o \omega^2 J \qquad (IV,5)$$

With simple harmonic flapping motion, the moment of thrust at the blade is therefore constant, independent of the angle of rotation. It is equal to the (constant) moment of the centrifugal forces set up as a result of the "coning motion."

With heavy blades, i.e., plane motion, as we shall assume them, $\beta_o \longrightarrow 0$ (fig. 9). Then M_s disappears also, compared with the other moments acting on the blade.

Now M_s must be expressed as function of the thrust.

Velocities and aerodynamic forces at the blade.- As in the section "Autogiro of Low Tip-Speed Ratio", page 12, the air stream (with respect to the plane at right angle to the axis of rotation) of the autogiro at angle α is represented by its components (fig. 9):

$$\text{Forward speed,} \quad v \cos \alpha = \lambda u,$$

$$\text{Axial velocity,} \quad v_d = \lambda_d u.$$

The forward speed in the normal plane is resolved for each ψ into its components along and perpendicular to the blade (fig. 10) which, together with the rotary motion, give the c_x and c_y components of the speed c relative to the blade element at right angle to the blade axis (c_y lies on the plane through the axis of rotation), according to figure 11 and with $\beta = \beta_1 \cos \psi$ at

$$\left.\begin{aligned} c_x &= c \cos \varphi = r \omega + \lambda u \sin \psi \\ c_y &= c \sin \varphi = \lambda_d u + \beta_1 \lambda u \cos^2 \psi - r \frac{d\beta}{dt} \end{aligned}\right\} \qquad (IV,6)$$

Apropos c_y, $\beta_1 \lambda u \cos^2 \psi$ is the component of $\lambda u \cos \psi$ (fig. 10) in direction of the blade axis, and $r \frac{d\beta}{dt}$ the perpendicular velocity produced by the flapping motion.

According to (IV,4) and figure 9:

$$\frac{d\beta}{dt} = \beta_1 \omega \sin \psi \qquad (IV,7)$$

It can be shown that the effect of this flapping motion is identical with a blade-angle change through

$$\Delta \vartheta = - \beta_1 \sin \psi,$$

when substituting for the "flapping" a "fixed" propeller whose axis of rotation relative to the first is inclined at β_1 to the rear. This is readily apparent from figure 9. Lock (reference 2) gives elaborate proof, deduces all formulas for both cases, and proves their identity.

Then we put, as before,

$$c_{ap} = \alpha_p \, c'_{ap},$$

so the thrust element at the blade of constant chord t becomes

$$d S = \frac{\rho}{2} c'_{ap} \, t \, dr \, \alpha_p \, c^2. \qquad (IV,7)$$

Again

$$\alpha_p = \varphi + \vartheta$$

at constant blade angle ϑ; consequently,

$$\alpha_p \, c^2 = (\varphi + \vartheta) \, c^2,$$

or with (IV,6), wherein $\sin \varphi = \varphi$ ($c_y = c \, \varphi$) and $\cos \varphi = 1$ ($c_x = c$):

$$\alpha_p \, c^2 = c_x \, c_y + \vartheta \, c^2.$$

Thus the thrust component becomes

$$d S = \frac{\rho}{2} c'_{ap} \, t \, dr \, (c_x \, c_y + \vartheta \, c^2) \qquad (IV,8)$$

The component of the tangential force is assessed in similar manner:

$$d T = - \frac{\rho}{2} t \, dr \, (c_{wp} \, c_x^2 - c'_{ap} \, \vartheta \, c_x \, c_y - c'_{ap} \, c_y^2) \qquad (IV,9)$$

Flapping angle, thrust, and coefficient of axial flow.- The subsequent stage of the analysis is explained on the very simple calculation of the flapping angle β_1. In the formula (IV,5) for the thrust moment of the flapping motion, we express M_s as sine series, stopping - as for β - after the first periodic term. Then

$$T_o - T_1 \sin \psi = \beta_o \omega^2 J.$$

Since there are no periodic terms at the right-hand side, the coefficient of $\sin \psi$ at the left, must become null. And β_1 is therefore obtained by writing the integral for M_s from (IV,1) with the aid of (IV, 6,7, and 8) and putting the sum of the terms with $\sin \psi$ equal to zero after integrating. The result is:

$$\beta_1 = 2 \left(\lambda_d + \frac{4}{3} \vartheta\right) \frac{\lambda}{1 - \frac{\lambda^2}{2}} \qquad (IV,10)$$

Similarly, the total thrust is:

$$S = \frac{\rho}{2} c'_{ap} \sigma u^2 F \left[\frac{\lambda_d}{2} + \frac{\vartheta}{3}\left(1 + \frac{3}{2}\lambda^2\right)\right] \qquad (IV,11)$$

and the coefficient of axial flow λ_d (by putting the moment = 0) from the sensibly symmetrical formula is

$$\frac{c_{wp}}{2\, c'_{ap}} (1 + \lambda^2) = \frac{\left[\lambda_d \dfrac{1 + \frac{3}{2}\lambda^2}{1 - \frac{1}{2}\lambda^2} + \dfrac{8}{3} \vartheta \dfrac{\lambda^2}{1 - \frac{1}{2}\lambda^2}\right]}{\left[\lambda_d \dfrac{1 + \frac{1}{2}\lambda^2}{1 - \frac{1}{2}\lambda^2} + \dfrac{2}{3} \vartheta \dfrac{1 + \frac{3}{2}\lambda^2}{1 - \frac{1}{2}\lambda^2}\right]} \qquad (IV,12)$$

These are Lock's formulas.

Comparison with model experiments.- This time the comparison is made unlike that in the section "The Autorotating Windmill", page 5. The test data for k_s* in

*From L_Ω after extrapolation:

$$k_s = 2 L_\Omega \sqrt{1 + \epsilon^2}.$$

reference 3 and the corresponding λ values (fig. 12) are written in the somewhat modified thrust formula (IV,11):

$$\lambda_d = \frac{2\,k_s}{\sigma\,c'_{ap}} - \frac{2}{3}\,\vartheta\left(1 + \frac{3}{2}\,\lambda^2\right) \qquad (IV,13)$$

wherefrom λ_d is defined. This permits the calculation of c_{wp} from (IV,12) (and at the same time renders the comparison independent of the induced flow, as explained elsewhere in this report).

The data shown in figure 13 are not readily interpretable, especially as concerns c_{wp}. To be sure, there already is a rather rational approximation to the anticipated amount at low λ (high α), but the steep rise at low α should, if it were real, be followed by a rise of λ_d for reasons of energy requirement (equation IV,15). The opposite is the case.

Aside from the values employed hereto, we also measured the flapping angles, i.e., the whole flapping motion was recorded with a small mirror attached at the blade root. The first thing noticed was that the actual blade motion differs very little from a simple harmonic oscillation and that the lateral inclination of the plane of rotation disregarded so far (the terms with $\sin\psi$), is vanishingly small. Of course, this close agreement is valid only for this particular model, whose massive wooden blades are dynamically unlike to actual design. Lock (reference 2) expresses the relation of aerodynamic force and contrifugal force by a nondimensional factor,

$$\gamma = \frac{\frac{\rho}{2}\,c'_{ap}\,t\,R^4}{J}\,. \qquad (IV,14)$$

According to his data on actually built autogiros, this ranges between 6 and 10, whereas the model shows $\gamma = 2$. Hence his blades are three to five times heavier than at full-scale. They strongly approach the ideal of the "heavy" blade, on which the calculations of this chapter are based.

To be sure, as soon as the computed amounts of flapping angle β_1 are compared with the measured values (fig. 14) the accord ceases. The computed β_1 are only about

two (thirds of the measured β_1, although the trend of the curves is still fairly the same; and a discrepancy as large as that cannot be explained away by inaccuracy in calculation or experiment.

Criticism of the assumptions.- The very fact of such a discrepancy in flapping angle β_1 goes to show that the thrust moment about the blade hinge producing the flapping motion could not have been correctly conceived. The mistake originates in the fact that the air strikes the retreating blade partly from the front and partly from the rear, thus producing angles of attack up to 180° along the blade. Obviously, the assumptions c'_{ap} = constant and c_{wp} = constant can no longer give even an approximately true picture, in that case,* by virtue of the practically complete breakdown of the flow across the whole blade.

In order to gain some idea of the magnitude of the error, we computed the thrust of a blade and its moment about the hinge axis for $\psi = 270°$, first according to formula (IV,8), then with the actual profile coefficients (Göttingen airfoil 429). (Because of the rapidly changing air-flow conditions the latter can, of course, also be considered only as approximate.)** The result is plotted in figure 15, in form of a thrust coefficient,

$$k_s = \frac{d\,S}{\frac{\rho}{2}\,t\,d\,r\,u^2}$$

and a moment coefficient

$$k_{ms} = k_s \frac{r}{R}$$

The difference (shaded portion) represents the margin of

---

*Lock (reference 2) himself states: "Finally, it may be worthwhile to attempt to meet the criticism, that in the analysis ... a structure is erected on the basis of the assumption 2 (namely $c_{ap} = c'_{ap}\,\alpha$, and c_{wp} = constant), which is too heavy for it to bear."

**Note at proofreading: Upon closer examination, it is found that the unsteadiness effects are numerically of no great consequence.

the computed over the actual moment, exceeding the latter by more than 50 percent.

Now, since according to the basic law (IV,5) of the flapping motion, the thrust moment shall remain constant during rotation, while on the other hand, the actual moment at $\psi = 270^\circ$ is much lower than the computed moment, the moment on the opposite side ($\psi = 90^\circ$), computed correctly because the α_p remain small there, must be reduced by an identical amount. That is, the blade must here intensify its upward motion $d\beta/dt$ to insure lower profile angle of attack. For reasons of symmetry the retreating blade follows this motion in inverse direction; but, operating as it does in practically separated attitude throughout, there is scarcely any change in thrust or moment. Consequently, it is the advancing blade which produces all or nearly all of this difference, and thus supplies the explanation for the discrepancy between the actually measured and the computed angles β_1.

It is hardly possible to express the actual behavior of the profile analytically by any relatively simple formula. Graphical representation with due allowance for the measured profile coefficients yields generally applicable results but only at great expense of time and labor. Thus there remains one alternative, and that is, to bring the mathematical integration data into relation with the "integral values" measured on the whole rotating wing. Then, we obtain with the data of figure 14, the approximation,

$$\beta_{1_{eff}} = a\,\beta_1 = 2\,a\left(\lambda_d + \frac{4}{3}\,\vartheta\right)\frac{\lambda}{1 - \frac{\lambda^2}{2}} \qquad (IV,15)$$

wherein $a \approx 1.5$ for $\vartheta = 0$, $a \approx 1.4$ for $\vartheta = 1.8^\circ$. The enumerator a obviously varies very little with the different blade angles, but may perhaps be very sensitive to changes in profile or characteristic. The rise in flapping angle must be so much greater as the lift curve is poorer and the maximum lift of the profile is lower.

The thrust of the individual blade at $\psi = 270^\circ$ is also a little lower than computed; owing to the accelerated flapping motion, it will equally be a little lower at $\psi = 90^\circ$. But opposed to this is an increment of the thrust quota of the blades lying in flight direction ($\psi = 0^\circ$ and 180°), for there the spatial air stream angles be-

come somewhat greater as a result of greater β_1. The ultimate predominating effect, however, can be decided only by elaborate graphical investigations.

On the tangential force* and its moment (fig. 16), the difference in trend and amount is especially conspicuous. The profound impelling moment appearing in the calculation at $\psi = 270^\circ$ does not exist at all in reality. This explains why, when evaluating the test data according to (IV,12 and 13), c_{wp} shows such a marked increase as λ increases without a contemporary rise of λ_d (fig. 13). The rotating power of the blade lift, greatly overestimated in the calculation of this part of the path, yields the apparent energy which must be equalized again by correspondingly higher profile drag. In reality, c_{wp} should not increase materially nor should λ_d decrease substantially.

The result of these investigations is the knowledge that the mathematical analysis of the processes on the autogiro of high tip-speed ratio is confined within comparatively narrow limits, which are due to the difficulty of reproducing the air force coefficients of the blade profile analytically correct and of accurately appreciating the flow phenomena involved at the blade.

In the following section it is shown that the hitherto accepted considerations themselves are in need of correction as regards their fundamental physical concepts.

THE INDUCED FIELD OF FLOW AND ITS EFFECTS

The airfoil of large chord.- In all considerations thus far the induced flow had been assumed at half the final deflection, in accord with Glauert and Lock (as detailed on page 14, on "Theory of thrust of the ideal autogiro." But, can this hypothesis which, according to Prandtl's airfoil theory, is limited to the simple lifting vortex, actually still be considered here as satisfactory approach?

And experiment is here also more convincing than all deliberations. The validity of the concept of lifting

*Actual $k_t = (c/u)^2 (c_{ap} \sin \varphi - c_{wp})$ with $c_{wp} = 0.012$ to $\alpha_p = 15^\circ$, then $k_t = 0$ (resultant at right angle to chord).

vortex for the airfoil of usual lift/drag ratio is corroborated by the fact that the lift increases linearly with the angle of attack and, upon conversion to different aspect ratio in accordance with Prandtl's formula, manifests a constant $dc_{ap}/d\alpha_p$, which is possible only when the field of flow is 2-dimensional. Now, experiments with very thick airfoils, particularly new American sections (reference 7), among which is an airfoil of circular plan form and similar profile (Clark Y) (see fig. 17), disclose for decreasing slenderness ratio, an increasing curvature of the lift curve which, compared to the straight lines obtained according to the simple theory of the lifting vortex, fall off continuously.

Consider, for example, the process on the circular airfoil: Visualize the airfoil divided into separate, transverse strips; that is, transformed, as it were, into a multiplane with wings spaced closely behind one another. The air flowing off from the most forward partial wing is already slightly deflected because of the lift production. It strikes the second wing broadside at a slightly smaller angle than the free flowing air to the right and left of it. Consequently, the flow within range of the second wing is already somewhat curved. The process continues over the chord and produces through the progressively increasing, yet consistently diminishing, deflection an unsymmetrical curvature in chord direction also. The field of flow must therefore be spatially curved, a kind of "saddle surface."

It can be inferred therefrom that the rear portion of the wing, particularly at low angles of attack, is under a smaller effective angle of attack than with plane flow.

The trend of the moment curve (fig. 17) bears this out. The moment about the focus (referred to a "mean" profile at lateral distance $4R/3\pi$ from the center) is, at low lift, substantially less than for the slender rectangular wing ($\Lambda = 6$). The foremost c.p. position is ~ 28 percent from the leading edge for the circular wing and ~ 39 percent for the rectangular wing with the same c_a (~ 0,45). The lift of the circular wing is therefore substantially closer to the leading edge, which may be viewed as an effect of the cited asymmetrical curvature of the flow in chord direction. (We shall not go into the peculiar stable behavior of the moment at higher c_a.)

To be sure, the airfoil of large chord has not been mathematically analyzed as yet. Fundamentally, the procedure will probably follow in support of the described process. Each of these partial wings would probably be replaced by a system of trailing vortices and the velocity field induced therefrom computed. But, as the circulation of every one of these partial wings will be affected by all the others, the calculation would become extremely complicated.

The position of the direct lifting propeller is even less hopeful. Whereas, with the fixed-wing, the division into separate rectilinearly bounded strips with constant $dc_a/d\alpha$ seems still possible, this strip method would be impossible to apply to the rotating wing; $dc_a/d\alpha$ would change from one point to the next. An investigation of this kind would call for expenditures out of all proportion to the gain derived from it. Hence a suitable approximation must suffice.

The "substitute" autogiro.- Since we must forego building up the field of flow from the differential, we must begin with the integral, i.e., with the experiment on the whole model and then draw conclusions a posteriori. Admittedly, such summary procedure affords only summary results. But a method which renders the processes at least correct as to type is always preferable to one which is patently wrong. Even if it does not completely answer the demands of physical exactness, it nevertheless gives the engineer some foundation upon which he can base his analysis with some measure of confidence.

The process of reasoning is as follows: The real lifting propeller is replaced by a substitute propeller without flapping motion, whose field of flow is readily computed; it inclines at α_d to the normal plane. The difference between the (measured) angle of attack α and the thus defined α_d is the induced inclination α_i of the flow.

Now what does the substitute propeller look like? Of course, it should have the same shape as the real one, in order to make the transition possible, but relative to its flow conditions, it should correspond to the lifting propeller with tip-speed ratio approaching zero, described in the section "Autogiro of Low Tip-Speed Ratio", page 12; that is, it should be tractable with the simple formulas derived there. The thrust coefficient k_s is to remain

unaltered. And the remarkable result - the inner justification of this procedure - is that the corresponding profile drag coefficients with this substitute are actually in quite close agreement with those anticipated from profile measurements, so that conversely, starting with profile measurements, reasonable figures can be obtained for the lifting propeller.*

From (III,11 and 14) we obtain:

$$\left.\begin{aligned} k_s &= \sigma\, c'_{ap} \left(\frac{\vartheta}{3} + \frac{\lambda_d}{2}\right) \\ \text{and} \qquad \lambda_d &= 2\left(\frac{k_s}{\sigma\, c'_{ap}} - \frac{\vartheta}{3}\right) \end{aligned}\right\} \qquad (V,1)$$

and

$$c_{wp} = 2\, c'_{ap}\, \lambda_d \left(\lambda_d + \frac{2}{3}\vartheta\right) \qquad (V,2)$$

The thrust coefficients k_s are taken from figure 12 as mean values in the pertinent range ($\alpha = 5^\circ$ to $\alpha = 15^\circ$); c'_{ap} is, as before, put = 5.6. Thus, we have:

ϑ =	0	1°	1.8°	1.8° (2 blades)
k_s =	0.016	0.0195	0.023	0.0115
λ_d =	0.030	0.025	0.022	0.022
100 c_{wp} =	1.0	1.03	1.08	1.08

The amounts of c_{wp} show the anticipated order of magnitude. For more exact comparison the profile lift figures at which the various propellers operate, should be taken into account. We introduce, according to Glauert (reference 1) a "mean" lift coefficient

$$\bar{c}_{ap} = \frac{3\, k_s}{\sigma} \qquad (V,3)$$

that is, the c_a at which all profiles of the rectangular blade would have to operate in order to give the same

*The reason for this, at first, astonishing result, lies probably in the fact that even at high tip-speed ratio the flow is still sound over the major portion of the propeller disk and that the portions with separated flow contribute little to the torque.

k_s.* The figures are:

ϑ =	0°	1°	1.8°	1.8° (2 blades)
$\bar{c}_{ap}$ =	0.25	0.30	0.36	0.36

At these lift figures our computed c_{wp} are accordingly 15 percent higher than the Göttingen measurements for $t = 0.2$ m, $v = 30$ m/s (fig. 8) which, as already stated, is about equivalent to the profile characteristics at 2/3 R. This discrepancy can be unqualifiedly explained by the thickened trailing edge and the probably slightly different surface roughness.

The transition to the whole autogiro is most conveniently accomplished by substituting the "ideal" autogiro (see page 12) for the "substitute" autogiro, which differs from the latter only in its constant axial velocity over the whole propeller disk.

The axial flow coefficient ζ can be expressed through (II,7 and 10) in terms of k_s and λ_d:

$$\zeta = \frac{4}{3\sqrt{2\sigma\frac{c_{ap}^3}{c_{wp}^2}}} = \frac{\frac{2}{3}c_p}{\sqrt{\frac{\sigma\, c_{ap}}{2}}},$$

whence $$\zeta = \frac{\lambda_d}{\sqrt{k_s}} \qquad (V,4)^{**}$$

The results for the four analyzed propellers are:

ϑ =	0°	1°	1.8°	1.8° (2 blades)
ζ =	0.240	0.178	0.148	0.208

*According to (II,7), $\bar{c}_{ap}$ is 1.5 times that of the constant c_{ap} for the lancet-shaped blades, which is connected with the definition of σ.

**Identical with equation (III,17), although (V,4) is generally valid, independent of blade form.

These axial flow figures are considerably lower than those computed in section, page 12. The rotor blades seem to be more solid, so to speak, because of the lower profile losses.

To establish the induced inclination, α_i of the flow on the "substitute," we revert to equation (III,6) and figure 6. Then

$$\alpha_i = \alpha - \alpha_d = \alpha - \frac{v_d}{v \cos \alpha} = \alpha - \frac{\zeta \sqrt{c_s}}{\cos \alpha}$$

or

$$\underline{\alpha_i = \alpha - \zeta \sqrt{c_s} \sec \alpha} \qquad (V,5)$$

The result of the model tests interpreted with this formula, is shown in figure 18. Incidental to this, it should be noted that:

α_i is the inclination of the "substitute" flow, that is, that plane flow yielding the same total propeller force as the actual, 3-dimensional curved flow. The degree of curvature obviously is bound up with the permeability of the autogiro.

This becomes especially clear with the limiting transition ($c_{wp} \longrightarrow 0$) to the "solid" propeller. Here no air passes through at any point. The thrust of each element of the propeller surface is given with the blade form and blade angle and independent of the adjacent elements. The induced flow must follow the plane propeller surface, that is, be plane itself within range of the propeller disk.

However, with the growing permeability continuously larger masses of air pass through the forward part of the propeller disk, are deflected there and lower the effective angle of flow of the rearward lying parts. Through this process the forward part of the propeller is, in consequence, more heavily loaded, the rate of deflection is more rapid, and the curvature in longitudinal direction will, as a result, be greater than in the rearmost part. The major portion of the propeller thus will operate because of this unsymmetrical curvature, in a flow which is already inclined at more than half of the ultimate angle of deflection $c_s/2$. Consequently, the plane substitute flow must incline at more than $c_s/4$.

It is seen how α_i and v_d are so much more closely coupled together as the permeability, expressed by ζ, becomes greater.

This is fully substantiated by figure 18. The greater ϑ is, the smaller ζ, and consequently, α_i also. The points for each of the three four-bladers lie sensibly on a straight line. The figures for the two-blader are, as expected, below those of the four-blader with equal ϑ, because of greater permeability. Admittedly, they spread more and also are lower than would correspond to the pertinent ζ. Perhaps there are boundary or discontinuity interferences in action on account of the small number of blades.

Owing to the small number of experiments available for the evaluation, it is difficult to decide whether the α_i lines actually are straight and to what extent ζ as well as λ (owing to the nonuniform lift distribution transverse to the flow) has any effect on α_i. Besides, it should be remembered that the matter becomes so much more uncertain as α is smaller. For, since the flapping angle increases (increase of λ) the agreement of the thrust of the "real" with the "substitute" propeller becomes consistently poorer. The real propeller probably still gives - if it has not already fallen out of step - a small positive thrust, even at $\alpha = 0$, which according to (V,5) would yield a negative α_i. This is, of course, impossible and thus exposes one fundamental defect of our analysis.

It would therefore serve, for the time being, no useful purpose to express the α_i lines conformably to figure 18 in mathematical form. What we lack are further model experiments at sufficiently large scale (and, as much as possible, in an open jet). Until then, the empirical relationship of figure 18 must suffice; intermediate figures are out of the question because of the excessively deviating forms.

Behavior of autogiro in curved field of flow.- The general applicability of our analytical method is contingent upon being cognizant of the fact that the field of flow can be curved considerably without affecting the integral of the thrust and of the moment, as already established by Glauert (reference 1) for a particular case. To explain the observed lateral components, he temporarily assumed a semicircular flow curvature which ensues when w

is allowed to increase evenly in chord direction from 0 to its ultimate value $v\ c_s/2$. He finds that this certainly exaggerated curvature does not affect thrust and moment when compared with the figures for plane flow whose inclination amounts to $c_s/4$. That such symmetrical, semicircular flow is impossible by virtue of the interaction of the forward part of the propeller on the rear part, has already been pointed out.

Now let us examine another kind of flow curvature. Anent the rectangular-blade propeller, we assumed v_d as constant across the propeller-disk area in first approach (see page 17), although the thrust loading adjacent to the tip is certainly higher than next to the hub; the difference increases with ϑ. And we already pointed out that time that the axial velocity next to the hub would be higher than away from it.*

To simplify matters, we chose a rectilinear outwardly decreasing distribution of the axial velocity of the form (fig. 19)**

$$v_d = v_{d_o}\left(1 - p\,\frac{r}{R}\right) \qquad (V,6)$$

This v_d must then be brought into relationship with the elsewhere used constant v_d; we write these quantities as mean values with a dash, thus:

$$\overline{\lambda_d} = \frac{\overline{v_d}}{u} \qquad (V,7)$$

The connection between these two terms is established by the physical condition that the total amount of air passing through per second be the same. This is equivalent to a constant mean angle of axial flow,

---

*Visualize the lifting propeller as having a big hole in the center, through which air passes unrestrictedly. In this manner the mutual interference of all parts of the propeller disk is knowingly disregarded.

**Together with forward speed $v \cos \alpha$, it gives for the field of flow a readily tractable 3-dimensionally curved surface.

$$\overline{\alpha_d} = \frac{\overline{v_d}}{v \cos \alpha} .$$

with equal total thrust and equal velocity.

Expressed in formula, the condition reads

$$\frac{\pi}{\overline{v_d}} = \frac{2\pi}{F} \int_0^R v_d \, r \, dr \qquad (V,8)$$

These three equations provide the assumptions for the calculation. According to (V,6) and (V,8), it is

$$\overline{v_d} = \frac{2\pi}{F} v_{d_o} \int_0^R \left(r - \frac{p}{R} r^2 \right) dr = v_{d_o} \left(1 - \frac{2}{3} p \right)$$

or, with v_{d_o} from (V,6):

$$v_d = \overline{v_d} \frac{1 - p \frac{r}{R}}{1 - \frac{2}{3} p} \qquad (V,9)$$

The velocity distribution of equal quantities of flow therefore have the point $r = \frac{2}{3} R$ in common (fig. 19). In this point the axial velocity corresponds to the constant v_d employed elsewhere. The most important part of the blade lies also in this vicinity. (See (II,10), page 10.)

Then we compute S and λ_d with (V,9), as before; the result is

$$S = \frac{\rho}{2} c'_{ap} \sigma u^2 F \left(\frac{\vartheta}{3} + \frac{\overline{\lambda_d}}{2} \right) \qquad (V,10)$$

or, exactly the same as formula (III,11). The thrust remains unaltered when putting $\lambda_d = \overline{\lambda_d}$, that is, the resultant amount of flow remains the same. The latter quantity is computed from the equation of definition:

$$\overline{\lambda_d}^2 \frac{6 - 8 p + 3 p^2}{\left(1 - \frac{2}{3} p \right)^2} + \overline{\lambda_d} \vartheta \frac{4 - 3 p}{1 - \frac{2}{3} p} - 3 \frac{c_{wp}}{c'_{ap}} = 0 \qquad (V,11)$$

As a check on the accuracy of the method, the 4-blade model with $\vartheta = 1.8^\circ$ was chosen, for which at v_d = con-

stant, the coefficient of axial flow was $\lambda_d = 0.022$. Instead of computing $\overline{\lambda_d}$ with given c_{wp} by variation of p, it is more convenient to define c_{wp} for $\overline{\lambda_d} = 0.022$ from (V,11). So long as c_{wp} remains constant, $\overline{\lambda_d}$ also would not change in the other case; but an increasing c_{wp} would have as counterpart a decreasing $\overline{\lambda_d}$.

Thus, (V,11) gives:

$$c_{wp} = 0.001 \frac{6 - 8\,p + 3\,p^2}{\left(1 - \frac{2}{3}\,p\right)^2} + 0.131 \frac{4 - 3\,p}{1 - \frac{2}{3}\,p} .$$

The result of varying p is shown in figure 20. $-c_{wp}$ remains sensibly constant from $p = 0$ to $p = 3/4$. The practical range of p must, by virtue of the equalization process, lie between $p = 0$ and the figure assumed for uniform thrust grading, estimated at $p = 4/5$ for the outer third of the blade with $\frac{dS}{dr}\frac{1}{r} = \text{constant}$. Accordingly, the actual value of p for $\vartheta = 1.8^\circ$ should lie in the neighborhood of 1/2 for minimum c_{wp}.

According to these examples, the distribution of v_d is not overly important as far as resultant thrust and resultant moment are concerned, provided the correct mean value of v_d has been attained. This fact assures us that the results of the foregoing section will not be much at variance with reality, even when the assumption $v_d = \text{constant}$ has not been wholly complied with.

THE LIFT/DRAG-RATIO CURVE (CHARACTERISTIC CURVE) OF THE AUTOGIRO

Origin and resolution of losses.- Heretofore the drag of the lifting propeller had been intentionally ignored, so as not to confuse the issue.

In the deductions for the autogiro of small tip-speed ratio (page 12) it was legitimate, for reasons of symmetry, to take the resultant thrust S at right angles to the plane of rotation, that is, in propeller axis direction. Its setting was at flow angle α_d to the inclined flow with induced angle α_i at the locus of the propel-

ler, in order to produce S. Then the component of S in the direction of undisturbed flow is

$$W_i + W_d = W_{sub} = S \sin \alpha \qquad (VI,1)$$

W_{sub} = drag of substitute autogiro, that is (according to the section "The Induced Field of Flow and Its Effects", page 30), of the autogiro characterized by identical form and thrust but vanishingly small tip-speed ratio.

The form of the polars is not suitable for plotting the drag of the autogiro, because the conditions are sensibly different from those of the fixed wing of the usual dimensions. The drags at high and low c_a are so utterly unlike, that a linear plotting would give only a very incomplete record of the figures at low c_a, where the best lift/drag ratios of the lifting propeller really lie. It is therefore better to plot the lift/drag ratio instead of the drag coefficient. Such a curve gives at the same time the drag of a lifting propeller of constant loading at the different operating attitudes.

According to the aforesaid, the lift/drag ratio of the substitute autogiro is with (V,5):

$$\epsilon_{sub} = \tan \alpha = \tan (\alpha_i + \zeta \sqrt{c_s} \sec \alpha) \qquad (VI,2)$$

with

$$\epsilon_i = \alpha_i \sec \alpha \quad \text{and} \quad \epsilon_d = \zeta \sqrt{c_s} \sec \alpha \qquad (VI,3)$$

for the region within which sin and arc may be interchanged; $\alpha_i \left(> \frac{c_s}{4}\right)$ results from figure 18, $\zeta = \frac{d}{\sqrt{k_s}}$ from equation (V,4). Both parts being dependent on c_s, it is preferable to plot against c_s rather than c_a; sec α is only a few percent higher than 1, hence can be estimated in design analyses.

Thus, the plotting of (VI,3) and the corresponding, measured values of the pertinent lifting propeller, gives a graphic view of the proportions of the losses at the lifting propeller (fig. 21). Apart from the two quotas, ϵ_i and ϵ_d, there is yet another, that due to nonuniformity, the asymmetry of the air flow at the blade on both sides of the median plane.

Nonuniformity losses.- Here we encounter the same difficulties experienced in the treatment of the flapping motion, to wit, a comparatively unwieldy and complex calculation can - owing to fundamental defects of the theorem - produce only moderately exact results. And the chief object of our mathematical analysis is to obtain a formula which then may be compared with the model measurements and adapted to them by a factor, as accomplished for the flapping angle β_1.

Lock (reference 2) defines the thrust component H perpendicular to the axis of rotation, in the same fashion as indicated in the section "The Autogiro of Large Tip-Speed Ratio - Flapping Motion", page 21, for β_1; the result can be formulated nondimensionally as effected for k_s:

$$k_h = \sigma \left[\frac{1}{2} \lambda c_{wp} - \frac{1}{2} \lambda c'_{ap} \lambda_d \vartheta + c'_{ap} \beta_1 \left(\frac{3}{4} \lambda_d + \frac{1}{3} \vartheta + \frac{1}{4} \lambda \beta_1 \right) \right] \qquad (VI,3)$$

Now we rewrite the equation so as to bring the quantity expressing the nonuniformity, that is, the tip-speed ratio λ_d, before the bracket. To this end, we remove β_1 by an approximation formula conformably to (IV,10):

$$\beta_1 = 2 \lambda \left(\lambda_d + \frac{4}{3} \right)$$

Then, with (VI,3), the lift/drag ratio of H becomes

$$\epsilon_u = \frac{k_h}{k_s} = \lambda \frac{\sigma c'_{ap}}{2 k_s} \left[2 \lambda^2 \left(\lambda_d + \frac{4}{3} \vartheta \right)^2 + \frac{c_{wp}}{c'_{ap}} + 3 \lambda_d^2 + \frac{13}{3} \lambda_d \vartheta + \frac{16}{9} \vartheta^2 \right] \qquad (VI,4)$$

which, after putting

$$3 \lambda_d^2 + 2 \lambda_d \vartheta = \frac{3}{2} \frac{c_{wp}}{c'_{ap}}$$

(according to (III,14), yields:

$$\epsilon_u = \lambda \frac{\sigma\, c'_{ap}}{k_s} \left[\lambda^2 \left(\lambda_d + \frac{4}{3}\vartheta \right)^2 + \frac{5}{4} \frac{c_{wp}}{c'_{ap}} + \frac{7}{6} \lambda_d \vartheta + \frac{8}{9} \vartheta^2 \right] \quad (VI,5)$$

And as a last step, we eliminate k_s through (V,1) and σ from (VI,5), so that

$$\epsilon_u = \lambda \frac{\left(\lambda_d + \frac{4}{3}\vartheta \right)^2 \lambda^2 + \frac{5}{4} \frac{c_{wp}}{c'_{ap}} + \frac{7}{6} \lambda_d \vartheta + \frac{8}{9} \vartheta^2}{\frac{\lambda_d}{2} + \frac{\vartheta}{3}} \quad (VI,6)$$

The numerical evaluation of this formula with the dimensions of the models manifests a rise in the value of the fraction (as a result of the effect of ϑ in the numerator) with ϑ (0.21 at $\vartheta = 1.8^\circ$ against 0.155 at $\vartheta = 0^\circ$), whereas the first term of the numerator with λ^2 is of no significance. But, according to a previous section (p. 21), the tangential force is much overestimated for the retreating blade; the overestimate increases with ϑ. Consequently, it may be expected that the value of the fraction in (VI,6) is a little lower and more constant than the calculation discloses.

To check this, we put

$$\epsilon_u = \kappa \lambda \quad (VI,7)$$

and define ϵ_u by trial insertion of different but constant values of κ for each model, so that the test points of the four models compared here are reproduced as closely as possible. As a matter of fact, this is surprisingly well accomplished, according to figures 22-25. The nonuniformity loss for each propeller in close approach is comparable to the tip-speed ratio.

But the enumerator κ also fluctuates only very little. Admittedly, it does not rise with ϑ as it should, according to (VI,6), but rather shows a slight drop. In (round) figures it amounts to:

$\vartheta =$	0°	1°	1.8°	1.8° (2 blades)
$\kappa =$	0.135	0.13	0.125	0.125

It is fortunate for the check on the reliability of our method that precisely the two practically most important four-bladers with $\vartheta = 1^{\circ}$ and 1.8° (of which the latter especially, shows numerous test points) are so closely and accurately expressed by the simple law (VI,7). But the enumerator of the two-blader (fig. 25) is difficult to define exactly, because the points scatter irregularly. Since, however, σ does not occur in (VI,6), we chose κ as for the corresponding four-blader. The curve passes through the middle of the test points.

During the evaluation it should be borne in mind that ϵ_u amounts to only a fraction, in part even a minor fraction of the total lift/drag ratio, so that errors in measurement in this enlarged by ϵ_u would be readily shown up. On the other hand, the accuracy of the measurements is limited by the fact that the deduction for the hub drag constitutes a considerable proportion of the total drag (23 percent for the four-blader with best lift/drag ratio and $\vartheta = 1.8^{\circ}$, and 39 percent for the two-blader). In spite of the fact that the hub drag had been measured separately with the greatest of care and with all due allowance for mutual interferences, the source for difficultly estimable inaccuracies still remains.

For this reason the data obtained from these experiments should not be considered as definite. Further model experiments at sufficiently large scale are urgently desired. But in the meantime, formula (VI,7) and the κ figures obtained here, may be confidently used. Whatever lack of accuracy the formula may have is more than balanced by its simplicity and practical convenience.

A somewhat deeper insight into the nature of nonuniformity loss ϵ_u may be gained by following Glauert's (reference 1) and Lock's (reference 2) procedure wherein, however, axial flow and nonuniformity losses $(\epsilon_d + \epsilon_u)$ do not occur separately. The power to be exerted by the profile drag of the blades in the propeller disk as used in section "The Autorotating Windmill", page 5, for computing the flow velocity, can equally well be resorted to for defining ϵ_u. Since the flapping motion as a kind of resonance oscillation absorbs no energy, there remains as lost power induced by the nonuniformity only the profile power.

The power due to uneven air flow equals the power of the corresponding drag proportion in path direction:

$$N_u = \epsilon_u A v.$$

Then with $A = S \cos \alpha$,

$$\epsilon_u = \frac{N_u}{v S \cos \alpha}.$$

Confining ourselves conformably to Lock (reference 2), to the velocity component c_x perpendicular to the blade axis (IV,6), we have:

$$N_u = \frac{\rho}{2} c_{wp} t \frac{z}{2\pi} \int_0^{2\pi} d\psi \int_0^R \left[(r\omega + \lambda u \sin\psi)^3 - (r\omega)^3\right] dr,$$

which, integrated, gives:

$$N_u = \frac{3}{8} \rho \lambda^2 c_{wp} z t R^4 \omega^3.$$

Then with (II,5), (III,2), and k_s in place of S, we have

$$\epsilon_u = 3 \frac{\sigma c_{wp}}{4 k_s} \lambda.$$

This agrees with the second part of the particular formula by Lock. Glauert computes the loss by including the component $\lambda_u \cos\psi$ in blade axis direction, that is, with the actual yawing velocity. The form of ϵ_u is retained hereby, the factor 3 becomes 4.5 (for $\lambda = 0$), or 5 (for $\lambda = 0.5$).

But the ultimate reduction has not yet been attained. It is accomplished by inserting k_s conformably to (V,1) and c_{wp} conformably to (V,4):

$$\underline{\epsilon_u = 3 \lambda_d \lambda \ (c_x \text{ only})}$$

and

$$\underline{\epsilon_u = (4.5 \text{ to } 5) \lambda_d \lambda \ (\text{actual air flow}).}$$

This result denotes that the losses on profile power increase with λ and (according to (II,10)) with ϵ_p as a result of uneven air flow.

The following tabulation gives the comparison with the experimental figures:

	$\vartheta = 0$	1	1.8°	
	$\lambda_d = 0.030$	0.025	0.022	
	$3\ \lambda_d = 0.090$	0.075	0.066	(c_x only)
	$5\ \lambda_d = 0.150$	0.125	0.110	(actual flow)
instead of	$\kappa = 0.135$	0.130	0.125	

The order of magnitude of the factors of λ is, to be sure, correct with a view to the actual air stream, but the change with ϑ is sensibly greater than with the model (κ). The fact of the factor for $\vartheta = 0$ becoming even greater than κ, is indicative of this method of calculation to overestimate the profile losses; for there probably is yet another unassessably small proportion to be added, as a result of the turbulence in the detached part of the flow at the retreating blade. So the actual value of the assessable profile losses probably lies between the two mathematical limits.

There is no doubt but that the lower limit ($3\ \lambda_d$) used by Lock as the starting point of his calculations, gives too favorable lift/drag ratios. Still, it would serve no useful purpose to speculatively form an additional term, say, by starting from ϑ, to establish the agreement with the measured κ. For that, the test data are not reliable enough yet. However, one fact is certain, and that is that the calculation with κ promises more reliable data by a simple method than any of the analytically adduced relations.

Practical importance of three-way division - Limitation.- Let us return to the diagrammatical representation of figure 21. We have seen that the energy loss at the lifting propeller expressed in lift/drag ratio can be resolved according to physical aspects into three components and assessed by approximation. They were:

a) the induced loss (ϵ_i); it has a lower limit, for which the induced angle of attack $\alpha_i = c_s/4$, but which is not reached in practice by virtue of the curvature of the flow. An approach is given

by subtracting the flow angle α_d from the angle of attack α on model experiments. The then obtained angle α_i (fig. 18) indicates the apparent slope of a plane field of flow, whose resultant effect on the propeller is the same as the actual curved field, which is difficult to assess numerically.

The induction loss on the lifting propeller is essentially given by the plan form, hence difficult to influence.

b) the flow loss (ϵ_d): It covers the power requirement by propeller rotation against the profile drag of the blades. Its relative minimum is obtained by assuming a tip-speed ratio approaching zero, i.e., symmetrical air flow; it is characterized by the axial flow coefficient ζ with flow angle.

$$\alpha_d = \zeta\sqrt{c_s} \sec \alpha \; (= \epsilon_d).$$

ζ is sensibly dependent on the lift-drag ratio of the profile at which the blade operates, and on the surface density σ; it can, therefore, be markedly influenced by the plan form.

c) nonuniformity loss (ϵ_u): It is a result of the uneven flow at the blades in the different settings with no longer negligibly small tip-speed ratio (as customary by energy conversion in flows of nonuniform velocity). Exact analytical assessment is probably impossible. In accord with model experiments, it can be expressed with

$$\epsilon_u = \kappa \lambda$$

where $\kappa = 1/8$ approximately for the usual range of blade angles. It can, like ζ, be influenced by the plan form.

The detailed process to be followed for reducing ϵ_d and ϵ_u is best seen when the formulas for the lancet-shaped propeller, developed in section, page 5, are used as basis.

A slightly modified (II,12) gives

$$\zeta = \frac{\frac{4}{3} c_{wp}}{2 \sigma c_{ap}^3} \qquad (VI,8)$$

and (II,13) together with (III,2 and 3) give

$$\lambda = \cos \alpha \sqrt{\frac{\sigma c_{ap}}{2 c_s}} \left(= \cos \alpha \sqrt{\frac{k_s}{c_s}} \right) \qquad (VI,9)$$

Of the three variables, c_{wp}, c_{ap}, and σ only the first appears with definite effect. The coefficient of axial flow behaves exactly like the drag coefficient of the blade profile. Contrariwise, c_{ap} and σ affect ζ in the inverse sense of λ; the greater $c_{ap}(\vartheta)$ and σ is, the smaller ζ becomes but λ, so much greater.

Formulas (VI,8) and (VI,9) show the designers of autogiros how to proceed in order to reach a particular aim.

On the other hand, it should be borne in mind that $c_{ap}(\vartheta)$ can only be increased to a limited extent. Up to now the evaluation of the model experiments had been intentionally limited to $\vartheta = 1.8^\circ$, although the measurements included blade angles of 2.3° and 3°. But the erratic behavior of k_s even at $\vartheta = 2.3^\circ$ was indicative of a marked irregularity of the happenings at the blade. Such measurements are unsuitable for checking or confirming a theory.

The data for $\vartheta = 2.3^\circ$ are included in figure 26. The improvement with great c_s as against $\vartheta = 1.8^\circ$ is slight, while the best values fall considerably behind. This is not simply due to the increasing λ conformably to (VI,10) for, upon closer examination, the enumerator κ in (VI,7) is also found to be substantially higher than with $\vartheta = 1.8^\circ$ ($\sim$ 0.145 against 0.125, increases with c_s). This example shows that a certain amount of care must be exercised in the application of our derivation method.

However, this much is certain: the smaller the tip-speed ratio, the more reliable our relationships. A low tip-speed ratio is attainable by small c_{ap} or σ with otherwise given conditions, but a certain percent change of c_{ap} vitiates ζ substantially more than an identical

change of σ. This is the reason why in high-speed aircraft, in which the nonuniformity loss is pronounced ($c_s < 0.05$), a low surface density is of advantage. Its inferior limit to-day is largely a design problem.

Any attempt at estimating the attainable ϵ encounters first of all c_{wp}, which for physical reasons constitutes an insuperable obstacle for any appreciable progress. In view of κ and λ together with the danger of falling out of step, it is imperative that c_{ap} in (VI,8) does not exceed a very limited amount while, on the other hand, σ should not become unlimitedly small, or else the flow loss at high c_s would become abnormally great and absorb too much power in climbing and throttle flight. The scope of improving c_{wp} under the conditions existing to-day is, indeed, very limited. It consists of careful selection and treatment of profile, higher characteristic through high tip speed, and fewer variations of c_{ap} through lower tip-speed ratios. And the total result of these attempts will at the very most, lower c_{wp} not to exceed 20 to 25 percent.

For computing the numerical values, the following formulas are used:

$$\epsilon_d = \frac{\lambda_d}{\lambda} \qquad \text{(VI,11)}^*$$

$$\epsilon_u = \kappa\lambda$$

ϵ_i is taken from figure 18, whereby

$$c_s = \frac{\cos^2\alpha}{\lambda^2} k_s \approx \frac{k_s}{\lambda^2} \qquad \text{(VI,12)}$$

λ_d, k_s, and ζ from (III,5), (V,1), and (V,4). To illustrate, for $\vartheta = 2^\circ$, $c_{wp} = 0.008$, and $\sigma = 0.08$, it gives

$$\lambda_d = 0.0173, \quad k_s = 0.0092, \quad \zeta = 0.18$$

and the ϵ values for high tip-speed ratio with $\kappa = 0.12$ (estimated from the test data with (VI,6) are:

---

*From formula (VI,3) with (V,4) and (VI,12).

λ	= 0.35	0.40	0.50
c_s	= 0.075	0.058	0.037
ϵ_i	= 0.028_5	0.023_5	0.017_5
ϵ_d	= 0.049_5	0.043	0.034_5
ϵ_u	= 0.042	0.048	0.060
ϵ	= 0.120	0.114_5	0.112

According to this, the ϵ value of the lifting propeller with rectangular blades will hardly exceed 0.10 even with the most favorable dimensions, especially since the coning motion (IV,14) will set up still other additional losses. On top of that there is the drag of the hub and of the other nonlifting parts (fuselage, landing gear), so that the ϵ value of the complete aircraft probably does not fall much short of 1/8.

As the best lift/drag ratio of the autogiro is not far from the maximum speed, it is not inferior, in this respect, at least, to the aircraft with a fixed-wing system. But in cruising flight, its lift/drag ratios are substantially less favorable, for which reason its use will probably always be limited to short and medium distance flying. And there its special advantages will come into full play: ease of handling, spinproof, indifference to gusts, and landing with steep angle of descent.

ADDENDA

The foregoing exposition is essentially limited to the purpose of assessing the aerodynamic quantities of the lifting propeller with a minimum of mathematics yet correct appreciation of the physical fundamental processes involved. Admittedly, they are in need of further improvement in many respects.

In the following, we select only a few of the more outstanding problems from the practical point of view.* To be sure, they will be more in the line of pointers and giving orders of magnitude than of adducing definite solutions.

---

*For general information on autogiros, see references 13 and 14.

Light and curved blades, cross-wind force.- In the developments thus far, the weight of the blades, or their centrifugal force, relative to the thrust had been assumed great enough so that the blade motion was sensibly in a plane. This still holds with sufficient approach for the mass conditions of the model where the recorded deviation from the plane, the angle of the coning motion, did not exceed 1 to 2°, which justified us in disregarding its effect.

But it is quite different with lifting propellers whose blades, as already pointed out in section, page 21, are quite often only from one third to one fifth as heavy as those of the model. Then the angle β_o of the coning motion is from 3 to 5 times as large as on the model. Its usual range is between 6 and 9°, and (IV,5) gives it the value*

$$\beta_o = \frac{M_s}{J\,\omega^2} \qquad \text{(VII,1)}$$

As the thrust moment M_s rises with the thrust, while it is proportional to ω^2, β_o is independent of the propeller loading and solely defined by the quantities ρ, c_{ap}, t, R, and J of (IV,14) and $c_{ap}(\vartheta)$.

Obviously, the coning form is not without influence on the propeller drag. The drag increment is primarily due to the accelerated air force of the forward blade ($\psi = 180°$) which has the greatest backward slope. Lock (reference 2) gives a general treatment of it in the second part of his report; and his formulas which, admittedly, must be used with certain reservations, give nevertheless, a measure of comparison. He finds for an autogiro with $\gamma = 10$ (as against 2 for the model), $\vartheta = 2°$, $c_{wp} = 0.012$, and $\sigma = 0.2$; that is, of slow speed and very light blades, that the best lift/drag ratio becomes about 0.0075 poorer.

But the coning motion has yet another effect: It explains the formation of a lateral inclination of the thrust which, without it, would be impossible. The advancing blade sustains, as we have seen, a far greater load

*Apart from the weight of the blades proper, which, however, plays an insignificant part in full-scale designs.

than the receding blade. As the resultant of the air force is consistently at right angles to the blade axis and this describes a cone, the other does likewise but, while revolving, changes its magnitude to such an extent as to set up a component perpendicular to the axis of rotation, which points athwart the direction of the retreating blade. According to Glauert's formula (reference 1), its ratio ϵ_s to the resultant force (a kind of lift-drag ratio) should be proportional to λ.

The curvature of the flow induces a second cross-wind force which, according to Glauert (reference 1) should be diametrically opposed to the first and increase with $1/\lambda$ (by camber of arc).

Lock's model experiments also include a lateral force measurement for the 4-blader at $\vartheta = 1.8^\circ$ (fig. 27). The force direction is indicative of its source from the coning motion, but the rise of its lift/drag ratio ϵ_s is greater than anticipated. This is probably bound up with the equally increased flapping motion (IV,15) compared to the theory.

Then the coning motion has yet a certain effect on the position of the cone formed by the blades. The forwardly accelerated air force (at $\psi = 180^\circ$) causes the blade to deflect, an additional flapping motion, which obtains in a displacement of the highest coning point of from 10 to 30° in the direction of rotation. Naturally this displacement affects, even if subordinately, again the magnitude of the lateral component.

The blade curvature effect ensuing with elastic blades under the combined effect of unevenly distributed thrust and centrifugal force loading is, in a certain sense, related to the just discussed process. Glauert and Lock assumed a mean curvature of the blade axis in circular arc form. Lock (reference 2) obtains for the aforementioned untoward dimensions and a 3-percent pitch of the arc, a drag increment of 0.011 for best lift/drag ratio.

But this result is the most uncertain of all, for the assumption of a constant curvature of blade axis is utterly untenable, as shall be shown hereinafter, because this point is of considerable importance for stress analyses.

Strength problems of the blade.- In the solution of

the question concerning the resultant air loads of the lifting propeller, we had, with success, taken advantage of the fact that the asymmetry of the air loads is amply equalized on both sides of the median plane. The correct resultant forces are obtained by simply assuming a "mean" symmetrical flow.

Such a method, however, breaks down in blade-stress analysis, because then it is a matter of maximum rather than of mean values. So, strictly speaking, we should equally be unable to have recourse to the simplified appreciation of a plane field of flow, but should know the actual flow at every instant. This, however, remains for the time being, but a pious wish because of the enormous mathematical difficulties involved.

And so there remains but one alternative for the stress analysis, namely, to start with a plane induced field of flow with the inclination α_i (fig. 18). Happily, this signifies, with the known equalization processes of such airfoil flows, an augmentation of the assumptions for the air loads, that is, added safety factor for the analysis; for at the points of greater operating angle, consequently greater locally produced thrust than agreeable to uniform thrust grading, the flow is more deflected and actually strikes the blade at a smaller angle than the calculation stipulates. Thus the highly loaded points are relieved and the lowly loaded, stressed more.

This consideration, while admittedly not universally valid, gives however the assurance in the majority of cases of being on the safe side. An exception might be the tip load of the forward lying blade at small angles of attack as a result of the relatively excessive flow curvature. That would have to be cleared up through measurements.

Now the situation of the load distribution of the blade in its four settings is basically as follows: On the straight blade the centrifugal force components normal to the blade cancel in every instance the mass forces produced by virtue of the flapping acceleration. Consequently, it suffices to analyze the play of the forces at the pure coning motion, that is, of the (constant and outwardly directed) centrifugal force and of the (variable and upward acting) air load.

So long as the blade is straight, the normal load increases linearly outward with uniform mass distribution

by virtue of the centrifugal force; but the air load increases rather parabolically outward at $\psi = 0$ and 180°. At this stage the moment of the load discrepancies bends the blade concavely upward. But at $\psi = 90^\circ$ the center of gravity of the air load shifts considerably to the inside and it may itself outwardly become negative under stated conditions. The blade is, as a result, severely bent concavely downward. Contrariwise, the air load shifts strongly outward at $\psi = 270^\circ$; the upwardly concave curvature should reach its maximum there. Thus the blade executes at each revolution a (not harmonic) forced vibration in bending. There is no imminent danger of resonance, since the frequency of first higher harmonics must be $> 2n$ by virtue of the ever-existing blade rigidity. Of course the air loads damp the motion of the individual blade elements again.

The ideal from the standpoint of strength would be a perfectly soft blade, a heavy rope, so to say, which at any instant conforms with the equilibrium of the external mass forces. Such an element would have to transmit longitudinal and transverse forces but no flexural moments. Naturally this is not feasible in view of the rigidity of the blade by nonrevolving rotor, and the designer is forced to some compromise relative to the desired stiffness. For the chosen stiffness and mass distribution, the normal loading is then established by progressive approach, the change of centrifugal force components due to varying blade curvature being of primary importance, followed by the change of air load. The first is directly dependent on the shape of the blade axis, the other on its first derivation with respect to time. A more exact examination of these processes involves an enormous amount of paper work, since no accurate short-cut method has been devised as yet.

Free-flight tests on the autogiro would make matters considerably easier. (There is no adequate wind tunnel in Europe where models at the desired scale could be tested.) The problem is twofold: a) determination of air loads at blade through pressure-distribution measurement at varying distance from the center; b) measurement of deflections along the blade axis.

Both problems present considerable experimental difficulties, because the measurements must be made on a rotating element which, in addition, is very sensitive dynamically as well as hydrodynamically. But they are defi-

nitely essential to completely clear up the conditions, especially with a view to the type of the induced field of flow.

Transition to very high angles of attack.- "The autogiro cannot be stalled." Undoubtedly this is true when referring to the flight characteristics; for the lift coefficient and the mean air-stream velocity of the individual blade element are in fact, as seen, independent of the angle of attack of the whole autogiro which therefore, does not lose its lifting power. But in spite of that the flow about the autogiro is not always so smooth as in the previously treated angle-of-attack range.

This is best seen in the picture of the axially impinged autogiro, the attitude of vertical descent, which has also been elaborately treated by Lock (reference 8), and Glauert (reference 9). The flow on the autorotating axially impinged propeller is analogous to the flow of a correspondingly impinged round disk, i.e., in front a symmetrical potential flow, behind it a turbulent zone separated by a more or less expressed inversion layer (area of discontinuity) from the potential flow. The fact that 10 to 20 percent of the flow escapes through the propeller disk on the autorotating propeller does not alter the picture decisively.

This flow, perfectly defined by the vortex field aft of the propeller, now must gradually change in the smooth airfoil flow as the angle of attack declines. The only attempt so far published which covers this whole range (reference 10), is illustrated in figure 28. The 4-blade model of 0.65 m (2.1 ft.) was tested in the 2.10 m (6.9 ft.) closed wind tunnel. The plot shows the lift curve anticipated for smooth flow conformable to (III,7) and (III,9), without particular regard to the induced flow.

The theory agrees very closely with the test data up to $\alpha = 15^{\circ}$ (fig. 29a). But at 20° the test points are already scattered,* a sign of disturbance of the smooth flow. Observations are still lacking regarding it, but it may be assumed that, analogously to the fixed-wing system, a dead air zone is formed on the upper side at whose

*In unlimited air stream the angle of incipient vorticity can be slightly higher.

release the eddying boundary layer of the individual blades will probably come into play. As a result the total flow will be accordingly less deflected (fig. 29) without necessarily inducing an appreciable effect of the sound flow at the individual blade element, for the eddy zone is not formed until above the plane of rotation. As the angle continues to increase, the flow around the leading edge will become more and more difficult, until at last the flow reverses altogether and approaches symmetrical form (see fig. 29c) observed at $\alpha = 90^\circ$ (reference 11).

Another step further leads to the following: According to Prandtl's airfoil theory, the lift of a wing of span b and identical deflection α_i at the locus of the wing can be equated to the momentum per second of an air mass passing at the rate v through a pipe section of diameter b and evenly deflected across the whole section by $2\alpha_i$, perpendicular to its mean direction. Then, as long as it is possible to make the flow pass along the surface of the lifting propeller without becoming separated, we have $\alpha_i = \alpha$ if the propeller is "dense" enough, and the fictitious pipe flow is deflected through 2α, that is, through 180° at $\alpha = 90^\circ$. In this case the propeller force coefficient would be $c_s = 4 \sin\alpha = 4$, according to (III,7). This is the highest, theoretically conceivable amount, according to the momentum theorem. (It corresponds to the perfectly elastic impact.*)

In reality, no such large deflection is realized: first, on account of the necessarily strong flow curvature within the propeller disk, which is not possible according to the mechanics of the propeller; then, it is diametrically opposed to the flow pattern observed at $\alpha = 90^\circ$, for which reason we have the incipient breakdown of the flow. Besides, the cited pipe does not deflect the whole mass flowing through it; part of it escapes beforehand, owing to the permeability of the propeller. The latter process is correctly assessed as to type through formula (III,9). On our propeller (fig. 28), it lowers the theoretical $c_{s_{max}}$ from 4 to 2.8.

Now the remarkable feature is that the measured $c_{s_{max}}$ is exactly half of this amount, that is, 1.4. If further experiments should confirm this result the cited Prandtl method could then be extended to include the perpendicularly impinged autorotating propeller, so far as the force could be computed from the same (fictitious)

pipe flow, with the proviso, however, that instead of 2α the total deflection angle would be only α, or $\alpha - \alpha_d$, that is, $90^\circ - \alpha_d$. This would give for the perfectly "dense" propeller ($\zeta = 0$) $c_{s_{max}} = 2$ as limit, in accord with Glauert's (reference 9) and Lock's (reference 8) curves extrapolated from the experimental values. This would bring us back to Newton, who deduced the same figure for the disk by means of his primitive momentum theory.

Assuming that it actually occurs: Why then does the round disk produce so much less drag ($c_w = 1.15$)? The difference can only lie in the form of the dead air space, that is, the vortex field in the wake of the disk. Whereas, on the fixed circular disk the air penetrates in the form of irregular, large balls, into the zone aft of the disk; the closely spaced vortex trains leaving the blade tips as helices on the lifting screw, should form a honeycomb-shaped envelope which prevents air from penetrating the dead air space, as well as from setting up any sufficiently large suction before the blade. The boundary layer flung off from the blades is probably very much involved herein. It should be worth while to explore this process thoroughly, especially by searching observation of the flow with smoke filaments.

This much may, however, be averred on the basis of modern knowledge, to wit, that the thrust coefficient will not be in excess of $c_s = 2$ in vertical descent - in most cases, even 20 to 30 percent lower. Higher figures observed here and there in free flight tests (reference 12) can be unrestrictedly explained by the almost always accompanying wind, which makes it easily appear as vertical descent when, as a matter of fact, it slopes perhaps 45°. In this case, for instance, the sinking speed would be only $1/\sqrt{2}$ times that of vertical descent; that is, the apparent air-force coefficient to be computed therefrom for vertical descent, would be twice as high as the actual.

In spite of that the drag of the autogiro in vertical descent is greater than that of a parachute. The remarkable fact is that this flight attitude with wing control is perfectly controllable, a characteristic in which the autogiro excels any other type of aircraft and which insures safe landing under the most difficult conditions.

SUMMARY AND CONCLUSIONS

It is shown that the flow on the autogiro in level flight can be reduced to the simple symmetrical flow on the axially impinged autorotating propeller. The unusually simple formulas set up yield not only the fundamental laws for flow and tip speed (section, page 5), but also a theory of the thrust of the autogiro which in form is in complete accord with the model experiments (section, page 12).

Discrepancies in the mathematical analysis of the thrust curves, however, point to the possibility of some fundamental error in the assumptions. But the effect of the asymmetry in the air stream, which effects the flapping motion of the individual blades, is described before this basic error is explained (section, page 21). It is shown that the mathematical treatment of these processes finds its comparatively narrow limits in the inadequacy of the formulas for the air forces at the receding blade. This is one reason why the English theory (references 1 and 2) could not produce satisfactory results despite the elaborate mathematical work.

The other reason lies in the assumption regarding the shape of the induced field of flow. The simple Prandtl assumption of a plane flow deflected by half the amount and valid for slender wings, must be altogether discarded. As the actual field of flow is scarcely tractable, a plane substitute flow is introduced whose slope is figured back from the model experiments (reference 3), whereby the real propeller is replaced by a substitute lifting propeller with symmetrical air flow. The latter gives drag coefficients for the blade profiles which agree with the Göttingen model experiments on the same wing section ("The Induced Field of Flow and Its Effects", page 30). It is shown that a moderate curvature of the field has no effect on the result, provided the plane substitute flow has been chosen correctly. Further model experiments with lifting propellers are urgently desired.

Then the total losses expressed in lift/drag ratio is resolved in three parts (see section, page 39):

a) induced loss (ϵ_i), always greater than $c_s/4$ empirically from figure 18 ($\epsilon_i = \alpha_i \sec \alpha$);

b) axial flow loss with a minimum of

$$\epsilon_d = \zeta \sqrt{c_s} \sec \alpha = \frac{\lambda_d}{\lambda}$$

whereby the flow coefficient ζ lies mostly between 0.12 and 0.25, and axial flow coefficient λ, also a constant (0.015 to 0.03), is sensibly defined from the profile lift/drag ratio;

c) nonuniformity loss $\epsilon_u = \kappa \lambda$, wherein κ, for good propellers, deviates apparently only a little from 1/8.

Since ϵ_d and ϵ_u depend inversely on the tip-speed ratio λ, whereas the induction loss is largely contingent upon the circular form, the improvement of total lift/drag ratio is within relatively narrow limits, about 1/10 with the usual form of to-day. The problem is essentially a matter of raising the speed by lowering the surface density and refinement in blade profile, propellers intended for high speed having narrower blades than those intended for good rate of climb.

The coning motion disregarded thus far, vitiates the lift/drag ratio very little, but sets up in conjunction with the curved flow, a lateral force which increases with the tip-speed ratio. (See section, page 49.) Our knowledge concerning it is still very incomplete.

The changing air forces deflect the blade during rotation, inharmonously upward and downward. The study of this process in flight measurements under simultaneous determination of the actual field of flow in the propeller disk is one of the most pressing problems (section, page 12).

In vertical descent the thrust coefficient c_s is about 50 percent of the value anticipated from the elementary theory. The amount of $c_s = 2$ is not exceeded (page 49). The flow breaks down when changing to high angles of attack, that is, relative to the total area, but remains sound at the individual blades, so that lifting power and controllability are maintained.

Translation by J. Vanier,
National Advisory Committee
for Aeronautics.

REFERENCES

1. Glauert, H.: A General Theory of the Autogyro. R. & M. No. 1111, British A.R.C., 1926.

2. Lock, C. N. H.: Further Development of Autogyro Theory. Parts I and II. R.& M. No. 1127, British A.R.C., 1927.

3. Lock, C. N. H., and Townend, H. C. H.: Wind Tunnel Experiments on a Model Autogyro at Small Angles of Incidence. R.& M. No. 1154, British A.R.C., 1928.

4. Cierva, Juan de la: The Development of the Autogiro. Roy. Aero. Soc. Jour., vol. 30, no. 181, pp. 8-29.

5. Hovgard: The Wilford Gyroplane. Aviation Engineering, September 1932.

6. Liebers, Fritz: Resonance Vibrations of Aircraft Propellers. T.M. No. 657, N.A.C.A., 1932.

7. Zimmerman, C. H.: Characteristics of Clark Y Airfoils of Small Aspect Ratios. T.R. No. 431, N.A.C.A., 1932.

8. Lock, C. N. H., Bateman, H., and Townend, H. C. H.: An Extension of the Vortex Theory of Airscrews with Applications to Airscrews of Small Pitch, Including Experimental Results. R.& M. No. 1014, British A.R.C., 1926.

9. Glauert, H.: The Analysis of Experimental Results in the Windmill Brake and Vortex Ring States of an Airscrew. R.& M. No. 1026, British A.R.C., 1926.

10. Caygill, L. E., and Woodward, A. E.: Wind Tunnel and Dropping Tests of Autogyro Models. R.& M. No. 1116, British A.R.C., 1926.

11. Lock, C. N. H.: Photographs of Streamers Illustrating the Flow around an Airscrew in the Vortex Ring State. R.& M. No. 1167, British A.R.C., 1928.

12. Cierva, Juan de la: The Autogiro. Roy. Aero. Soc. Jour., 1930, p. 902.

13. Schrenk, M.: Das Drehflügel-Flugzeug. Z.V.D.I., vol. 76, 1932, p. 843.

14. Schrenk, M.: Entwicklungsrichtungen im gegenwärtigen Flugzeugbau. W.G.L., December 14, 1932; Z.F.M., vol. 24, no. 10, 1933.

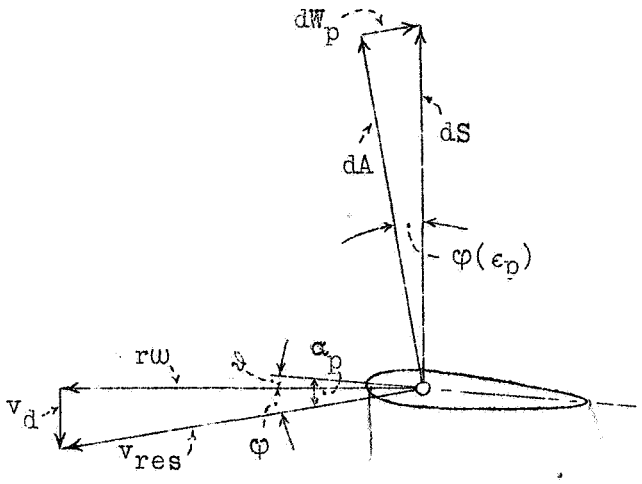

Figure 1.-Air flow and forces on the autorotating "elementary propeller" in equilibrium attitude.

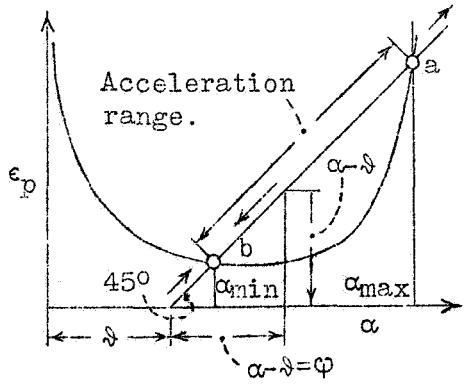

Figure 2.-Autorotation.range.

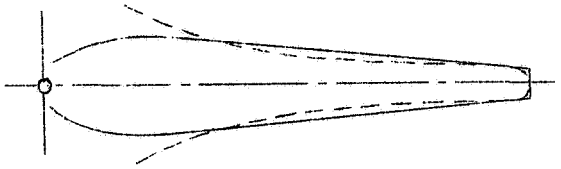

Figure 3.-Blade form of "ideal" autogiro. (lancet shape). The dotted lines are the plan form assumed in the analysis. The solid lines represent a practically feasible blade form, which in effect is little different from the other.

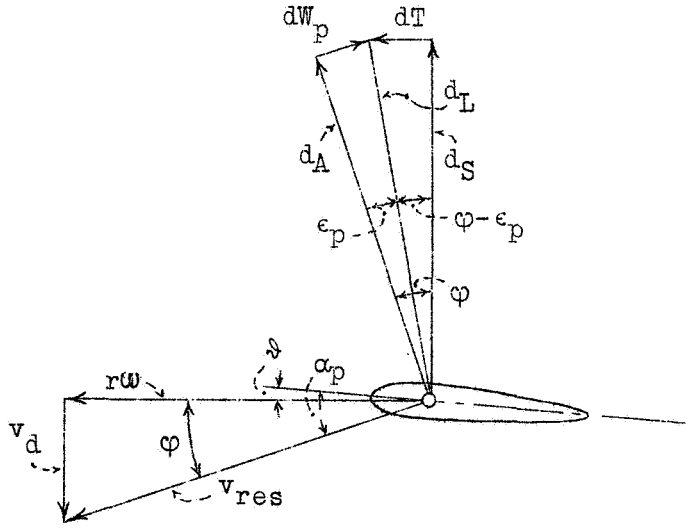

Figure 4.-Air flow and forces at blade element of autorotating lifting propeller.

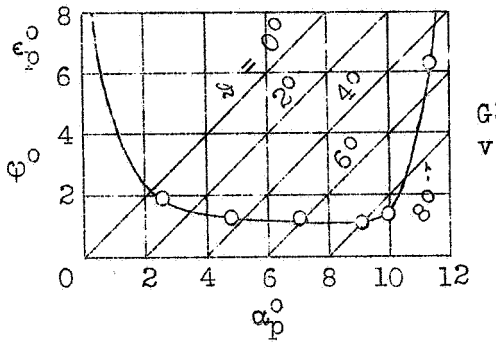

Figure 5.-Autorotation range for the lancet propeller with Göttingen 429 profile in axial air flow.

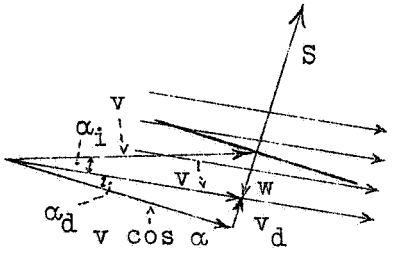

Figure 6.-Section through autogiro in level flight. Velocity v' in disk is composed of velocity v of undisturbed flow by deflection through angle α_i. The air passes through the disk at angle α_d.

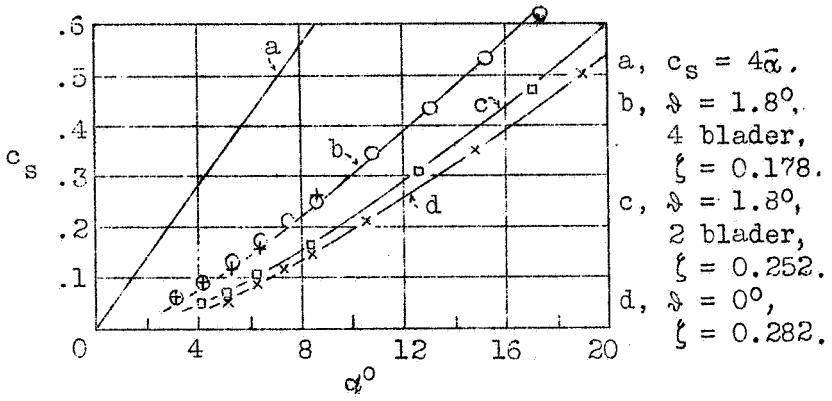

Figure 7.-Resultant force coefficient versus α for several autogiros. The points are measured, the curves computed according to theory of the autogiro with tip-speed ratio approaching zero. The agreement is exceptionally close. The straight line $c_s = 4\alpha$ gives the angle of deflection conformably to the theory of the lifting vortex.

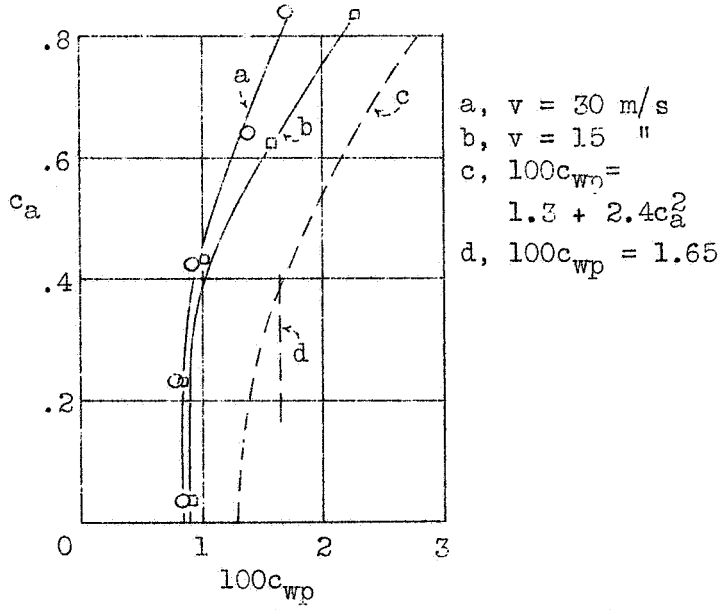

Figure 8.-Profile drag of Göttingen 429. The dotted lines refer to the mathematical data of section III, 6. The disagreement is obvious.

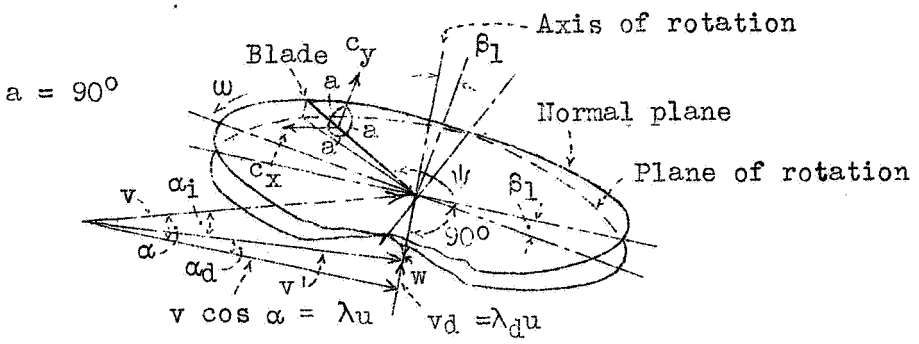

Figure 9.-Definition of flapping motion and ensuing velocities. The "heavy" blade runs at high tip-speed ratio, because of asymmetrical air flow in a plane (plane of rotation) inclined at angle β_1 to the normal plane. The transition from velocities v in the principal plane to the velocities c at the blade is effected by means of figs. 10 and 11.

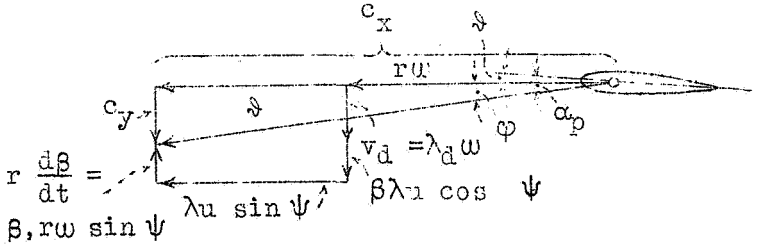

Figure 11.-Velocities at the flapping blade element.

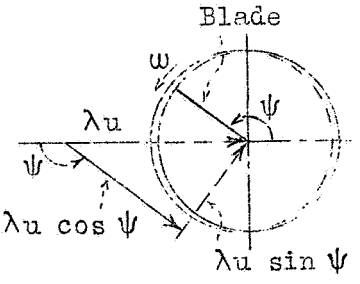

Figure 10.-Velocity distribution in the normal plane.

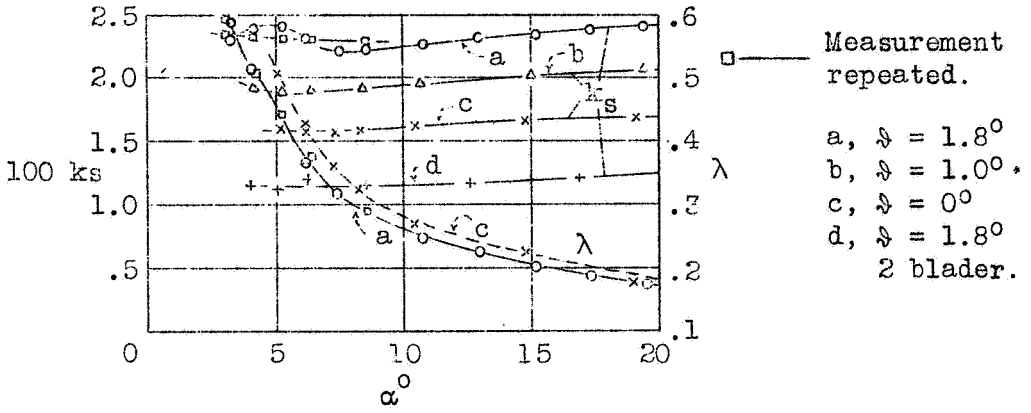

Figure 12.-Thrust coefficient and tip-speed ratio of the compared model measurements. The thrust coefficients are sensibly constant, those of the two and four blader of equal blade angle ϑ are in the ratio of 1:2.

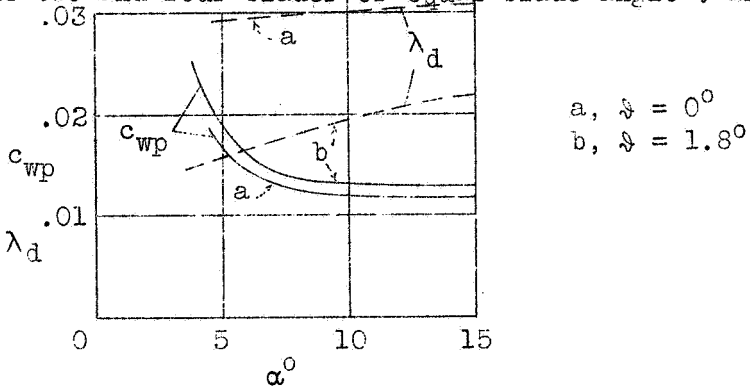

Figure 13.-Profile drag and coefficient of axial flow according to (IV, 12 and 13). The steep rise of c_{wp} at small α has no physical basis.

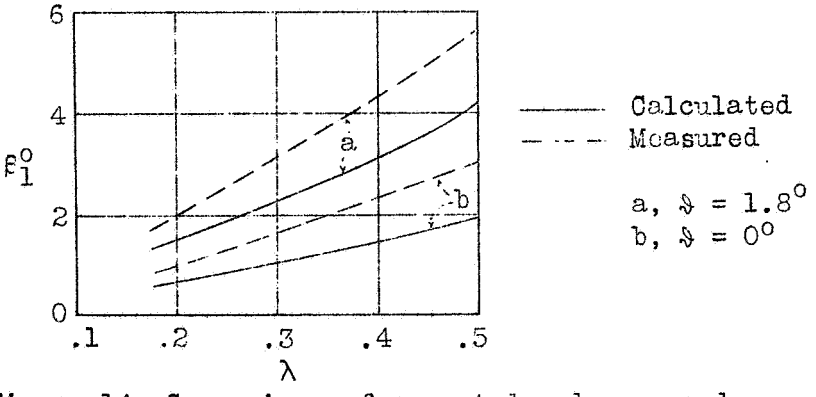

Figure 14.-Comparison of computed and measured flapping angles β_1.

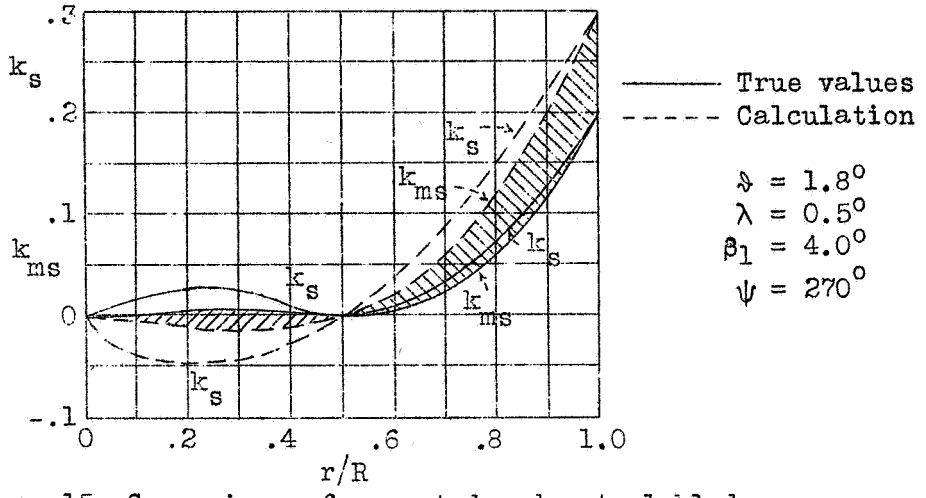

Figure 15.-Comparison of computed and actual blade thrust and its moment at $\psi = 270^o$.

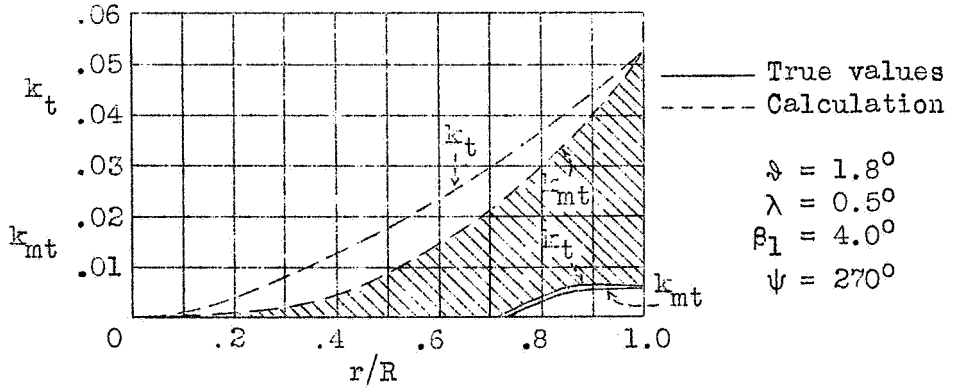

Figure 16.-Comparison of computed and actual tangential force and its moment at $\psi = 270^o$. The shaded area represents (at 5x scale of fig. 15) the excess of the computed over the actual moment of the tangential force about the axis of rotation. The actual moment is infinitesimal small.

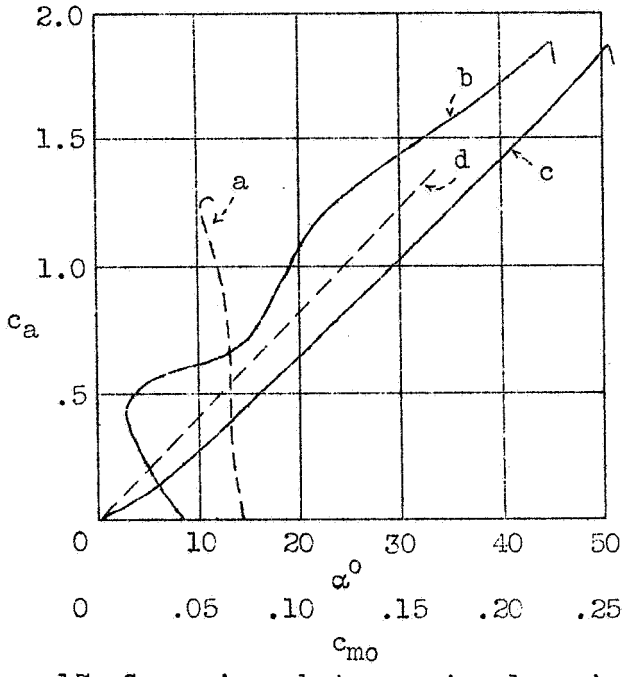

a, c_{mo} ($\Lambda = 6$)
b, c_{mo} (rotating wing)
c, $c_a(\alpha)$ (measurement)
d, $c = 2.35\,\hat{\alpha}$ lifting vortex.

Figure 17.-Comparison between circular wing and rectangular wing of equal profile (Clark Y).

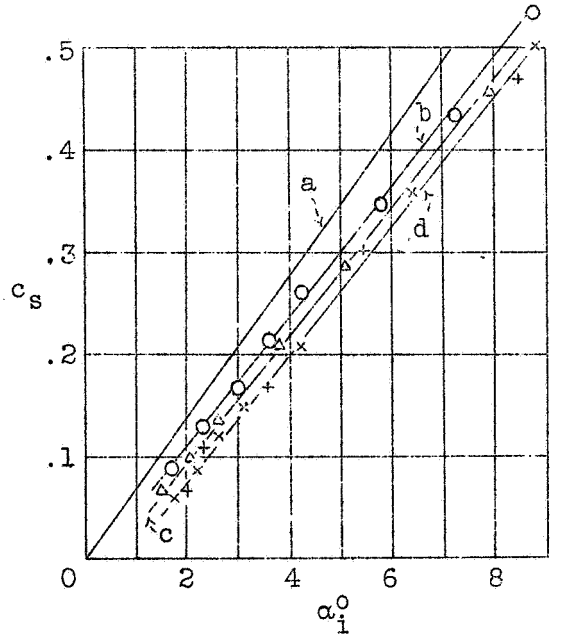

a, $c_s = 4\,\hat{\alpha}_i$
b, $\varphi = 1.8^o$ ($\zeta \approx 0.15$)
c, $\varphi = 1^o$ ($\zeta \approx 0.18$)
d, $\varphi = 0^o$ ($\zeta \approx 0.24$)

× $\varphi = 0^o$
△ $\varphi = 1^o$
○ $\varphi = 1.8^o$
\+ $\varphi = 1.8^o$ (2 blader)

Figure 18.-Induced inclination of the plane "substitute" flow at the locus of the lifting propeller.

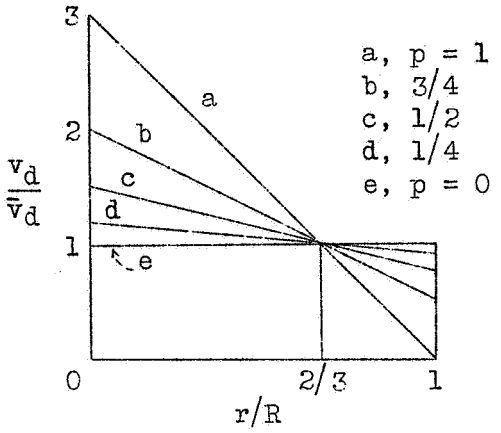

Figure 19.-Resolution of flow velocity along the radius.

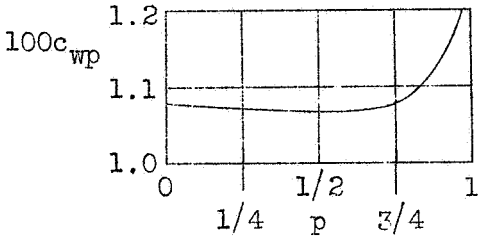

Figure 20.-Resolution of flow velocity plotted against profile drag coefficient.

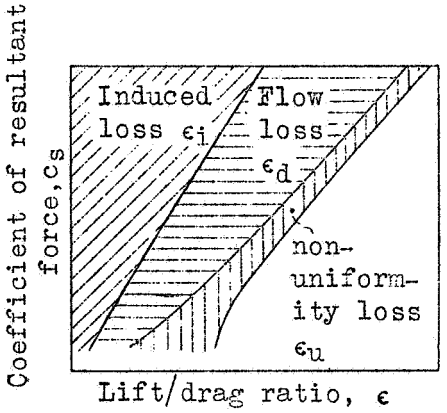

Figure 21.-Resolution of losses on the autogiro.

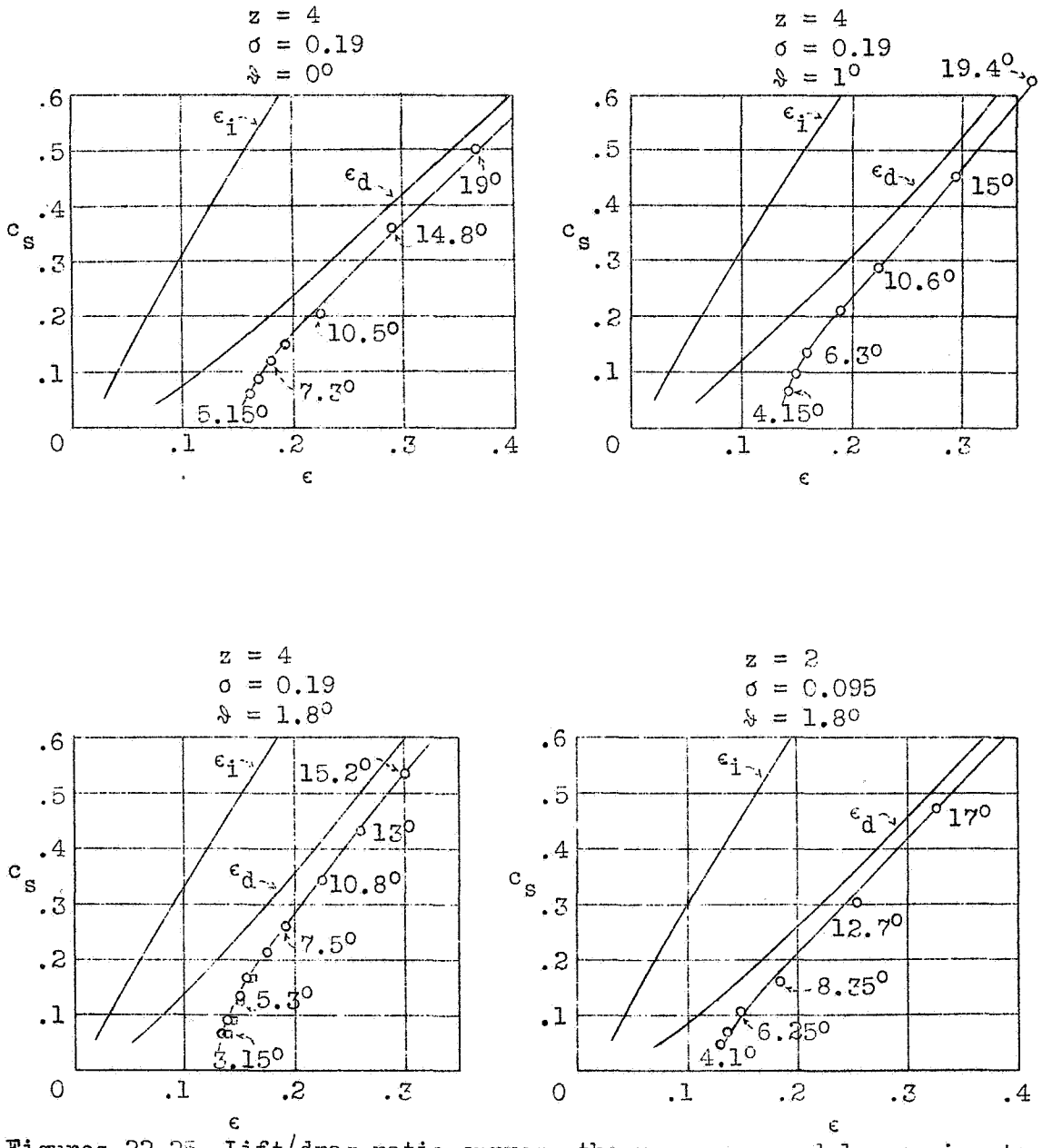

Figures 22-25.-Lift/drag ratio curves; theory versus model experiments.

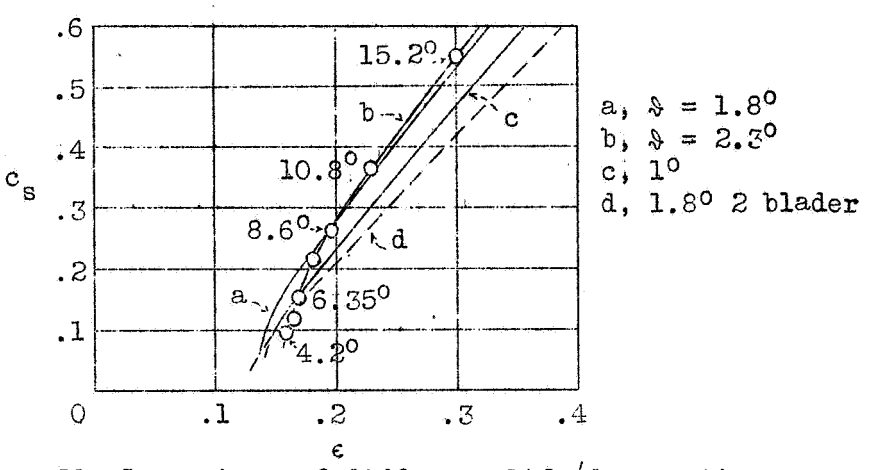

Figure 26.-Comparison of different lift/drag ratio curves, the behavior of ϵ for δ = 2.3°, shows that this latter measurement is not suitable for comparison with the theory.

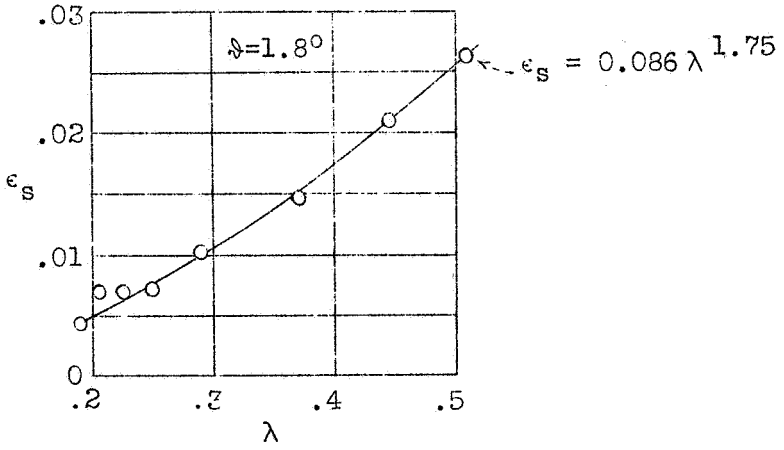

Figure 27.-Slope of lateral force for δ = 1.8°. This slope, expressed as a kind of lift/drag ratio is a power function of λ.

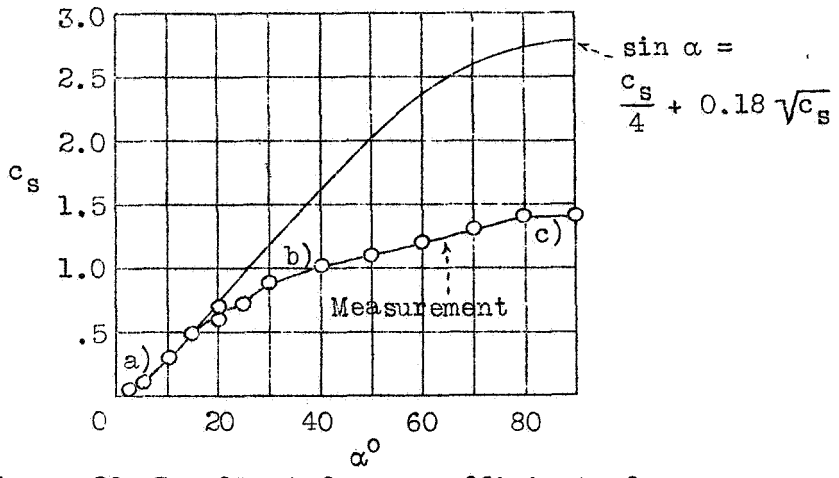

Figure 28.-Resultant force coefficient of an autogiro from 0° to 90°, compared with the simple theory. The flow at the propeller disk breaks down between 15 and 20°, the highest attained value of the total force coefficient is about 50 percent of the theoretical maximum. The letters a) to c) refer to the flow attitudes of fig. 29.

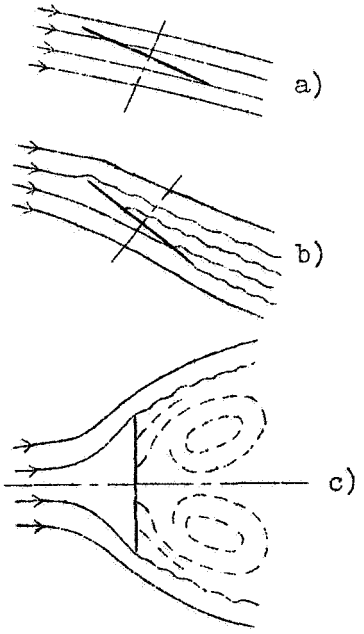

Figure 29.-Flow at autogiro for three different angles of attack. a) small angle of attack (up to about 20°) sound flow. b) medium angle of attack, flow broken down on propeller disk but still sound at individual blade. c) angle of attack 90°, symmetrical flow form, large dead air space aft of propeller disk, but flow still sound at individual blade.